European Journal of Taxonomy 1022: 202–242
https://doi.org/10.5852/ejt.2025.1022.3089
europeanjournaloftaxonomy.eu
ISSN 2118-9773
2025 · González-Ramírez M. *et al.*

Received: 6 June 2024 • *Accepted: 10 July 2025* • *Published: 13 October 2025*
Topic editor: Tony Robillard • *Section editor: Maxwell Barclay* • *Desk editor: Pepe Fernández*

Research article

urn:lsid:zoobank.org:pub:C59EC983-051A-42BD-A0B6-01DEBAC2F607

A phylogenetic analysis based on morphology reveals the placement of *Lycomesus* Zaragoza-Caballero & González-Ramírez, 2019 and *Lyconotus* Green, 1949 within Lycini (Coleoptera: Lycidae), with the description of a new genus from North America

Mireya GONZÁLEZ-RAMÍREZ [1,*], Santiago ZARAGOZA-CABALLERO [2], Juan J. MORRONE [3] & Helga OCHOTERENA-BOOTH [4]

[1] Posgrado en Ciencias Biológicas, Universidad Nacional Autónoma de México, 04510 Mexico City, Mexico.
[1,2] Laboratorio de Entomología, Departamento de Zoología, Instituto de Biología, Universidad Nacional Autónoma de México, 04510 Mexico City, Mexico.
[3] Museo de Zoología "Alfonso L. Herrera", Departamento de Biología Evolutiva, Facultad de Ciencias, Universidad Nacional Autónoma de México, 04510 Mexico City, Mexico.
[4] Departamento de Botánica, Instituto de Biología, Universidad Nacional Autónoma de México, 04510 Mexico City, Mexico.

[*] Corresponding author: mireya.biol@gmail.com
[2] Email: zaragoza@ib.unam.mx
[3] Email: morrone@ciencias.unam.mx
[4] Email: helga@ib.unam.mx

Abstract. Lycini are a species-rich tribe within the Lycinae, which are distributed across all biogeographic regions worldwide. Current classification of Lycini has been based exclusively on molecular evidence, and the North American species have been poorly represented. The placement of *Lycomesus* Zaragoza-Caballero & González-Ramírez, 2019 and *Lyconotus* Green, 1949 remains uncertain. In order to elucidate the phylogenetic position of these genera within the North American genera and to propose morphological characters that support them, we conducted phylogenetic analyses using parsimony and model-based approaches. Our morphology-based dataset included 91 adult characters from representatives of five genera and 33 species of the Lycini genera of the New and Old Worlds. We propose a new classification of the North American Lycini, consistent with the phylogenetic hypotheses. This includes the following taxa: *Lycomesus* Zaragoza-Caballero & González-Ramírez, 2019, *Lyconotus* Green, 1949 stat. rev., *Lycorectus* González-Ramírez & Zaragoza-Caballero gen. nov., *Neolycus* Bourgeois, 1883 and *Rhyncheros* LeConte, 1881. Additionally, we provide a key and diagnoses for all North American Lycini genera, as well as the morphological characters of males and females that define these genera. Our results indicate the necessity for a phylogenetic analysis that incorporates South American Lycini. This will enable a more precise generic classification of American Lycini.

Keywords. Net-winged beetle, Lycinae, taxonomy, Nearctic region, Neotropical region.

González-Ramírez M., Zaragoza-Caballero S., Morrone J.J. & Ochoterena-Booth J. 2025. A phylogenetic analysis based on morphology reveals the placement of *Lycomesus* Zaragoza-Caballero & González-Ramírez, 2019 and *Lyconotus* Green, 1949 within Lycini (Coleoptera: Lycidae), with the description of a new genus from North America. *European Journal of Taxonomy* 1022: 202–242.
https://doi.org/10.5852/ejt.2025.1022.3089

Introduction

Lycini Laporte, 1836 are the most diverse tribe within the subfamily Lycinae Laporte, 1836, with eight genera and more than 400 described species (Kusy *et al.* 2020). Lycines can be distinguished from other lycids by the elongated head forming a 'rostrum'; slender mandibles; antennomeres 3–10 flat, serrate to parallel-sided; elytra slightly to distinctly broadened posteriorly; spoon-shaped phallobase; and long and slender phallus (LeConte 1881; Green 1949; Zaragoza-Caballero 1995; Bocak & Bocakova 2008; Kusy *et al.* 2019, 2020). The tribe has a wide distribution, in almost all biogeographical regions of the world except the Antarctic (Gorham 1880; Kleine 1933; Blackwelder 1945; Green 1949; Bocak & Bocakova 2008; Masek *et al.* 2018). It has been proposed that they originally evolved in the southern part of the Nearctic region and Mesoamerica and later dispersed to Eastern Asia (Masek *et al.* 2018; Kusy *et al.* 2020). Despite their hypothesized American origin, approximately 70% of species are found in the Afrotropical region (Masek *et al.* 2018; Kusy *et al.* 2020). In contrast, only 7.6% of their diversity is reported in the Nearctic and Neotropical regions, with only four genera represented (*Celiasis* Laporte, 1840, *Rhyncheros* LeConte, 1881, *Neolycus* Bourgeois, 1883 and *Lycomesus* Zaragoza-Caballero & González-Ramírez, 2019) and 45 species reported for the region (Chevrolat 1834; Gorham 1880; Kleine 1933; Blackwelder 1945; Green 1949; Zaragoza-Caballero 1995; Pérez-Hernández *et al.* 2019; Zaragoza-Caballero & González-Ramírez 2019; Kusy *et al.* 2020). The genus *Celiasis* is reported in the literature to be endemic to Colombia (Gorham 1880; Kleine 1933; Blackwelder 1945). Since the type species could not be found, previous researchers dealing with this taxon (Kusy *et al.* 2020) could not study it, and this taxon is now considered a nomen dubium (Evenhuis 2012; Kusy *et al.* 2020). Bourgeois (1906), however, proposed that *Celiasis mirabilis* Lacordaire, 1857 (the type species of *Celiasis*) is not a lycid, but rather belongs to a genus of lycidiform melyrids that was later described by Blanchard under the name *Chalcas* Blanchard, 1845 (*Ch. trabeatus* Fairmaire, 1847). Despite the compelling story and rationale by Bourgeois (1906), *Celiasis* remain a nomen dubium in Lycini until the South American lineages are treated in the future. Furthermore, studies addressing the taxonomy of American genera have been limited. Consequently, authors often offer only cursory discussions on the morphology of the taxa studied (Chevrolat 1834; Melsheimer 1846; Dugès 1878; Gorham 1880, 1884; LeConte 1881; Green 1949).

Little informative descriptions, ambiguous taxonomic delimitations of genera and subgenera without a phylogenetic context, and inaccessibility of type material (Bourgeois 1883; Pic 1922; Kusy *et al.* 2020) have hindered the systematic work on the Lycini fauna worldwide (Kusy *et al.* 2020). In the New World, research on Lycini has been limited, with the majority of work focusing on catalogues, new species descriptions, checklists, and immature stages descriptions (Chevrolat 1834; Gorham 1880; Dugès 1896; Kleine 1933; Blackwelder 1945; Green 1949; Zaragoza-Caballero & González-Ramírez 2019; Pérez-Hernández *et al.* 2019; González-Ramírez & Zaragoza-Caballero 2024). Recently, Kusy *et al.* (2020) proposed a new genus-level arrangement of lycines based on a molecular phylogenetic analysis that included approximately 100 species. Their classification includes seven genera (*Celiasis*, *Neolycus*, *Rhyncheros*, *Lipermes* Waterhouse, 1879, *Haplolycus* Bourgeois, 1883, *Lycostomus* Motschulsky, 1861 and *Lycus* Fabricius, 1787). Kusy *et al.* (2020) separated the Old and New World species and treated *Lyconotus* Green, 1949 as a synonym of *Rhyncheros*. Despite the important contributions in this work,

the North American species of Lycini were underrepresented in their study, and the generic assignment of *Lycomesus* and *Lyconotus* raised several questions.

In order to contribute to the knowledge of the tribe and to evaluate the phylogenetic relationships of the North American Lycini, we conducted a phylogenetic analysis with dense taxon sampling aimed to encompass the largest number of genera and species from North and South America. Our objectives are to test the monophyly of Lycini, to clarify the phylogenetic relationships of North American genera, and to propose a classification consistent with the phylogenetic hypothesis. Finally, we utilize the results obtained to define the diagnostic characters of North American genera of Lycini, with which a dichotomous key has been constructed. Additionally, a diagnosis of the genera is presented.

Material and methods

Taxon sampling

Forty species were included in the phylogenetic analysis (Table 1). The ingroup consisted of 29 nominal species of Lycini and four undescribed species belonging to five genera (*Lycomesus*, *Lycostomus*, *Lycus*, *Neolycus* and *Rhyncheros*). The outgroup was represented by six species of the tribe Calopterini Green, 1949, which is considered to be more closely related to Lycini (Bocak & Matsuda 2003). For rooting the cladogram, we used a more distantly related species, *Chauliognathus* sp. (Cantharidae).

Repositories

A total of 1060 specimens (Supp. file 1) from the following collections (curators in parentheses) were analyzed.

ANSP = Academy of Natural Sciences, Philadelphia, USA (Jon Gelhaus)
CAS = California Academy of Sciences, California, San Francisco, USA (Chris Grinter)
CNIN = Colección Nacional de Insectos, Instituto de Biología, UNAM, Mexico City (Santiago Zaragoza Caballero)
NHMUK = Natural History Museum, London, UK (Michael Geiser)

Due to the lack of suitable material, the character coding for the male of *Lyconotus lateralis* (Melsheimer, 1846) was based on information obtained from the original description (Melsheimer 1846) and Green (1949); the coding of the female of *Lycus trabeatus* Guérin-Méneville, 1835, *Rhyncheros godmani* (Gorham, 1880), *Rhyncheros nigrofumosus* (Hinton, 1933), and the male of *Neolycus carmelitus* (Gorham, 1880) was based on photographs of the type specimens held at the NHMUK and CAS; the coding of the male of *Lycostomus praeustus* Fabricius, 1792 was based on the information provided by Kazantsev (2003); and the coding for the female of *Rhyncheros sanguinipennis* Say, 1823 was based on photographs of specimens from the ANSP (the acronyms CNIN, and ANSP follow the Insect and Spider Collections of the World website [Evenhuis 2023]).

Characters

All examined specimens were studied using a Zeiss Discovery V8 stereo microscope equipped with an ocular micrometer that was used for measurements. Genitalia were dissected and the surplus tissue was macerated using 10% KOH for 5 minutes. The wing morphology nomenclature and interpretation are based on Lawrence *et al.* (2021), and we followed Kazantsev (2003) for the female genitalia descriptions.

Due to the complexity to appropriately codify character states of characters 70 (paramere shape in lateral view) and 72 (phallus shape), we conducted a geometrical morphometric analysis using a representative 'normal' sample and one image per species, all using the same position and scale (Vega-Badillo *et al.* 2021). Photographs were captured with a Zeiss Axio Zoom V16 microscope with an Axiocam

Table 1 (continued on next page). Taxon sampling, with indication of the country.

Family	Tribe	Species	Country
	Ingroup		
Lycidae	Lycini	*Lycomesus llorentei* Zaragoza-Caballero & González-Ramírez, 2019	Mexico
		Lycus ampliatus (Fåhraeus, 1851)	South Africa
		Lycus trabeatus Guérin-Méneville, 1835	Burkina Faso
		Lycostomus praeustus Fabricius, 1792	India
		Lycostomus rubrocinctus Fairmaire, 1886	China
		Neolycus arizonensis (Green, 1949)	Mexico and USA
		Neolycus carmelitus (Gorham, 1880)	Mexico
		Neolycus fernandezi (Dugès, 1878)	Mexico and USA
		Neolycus lecontei (Green, 1949)	Mexico
		Neolycus sallaei (Gorham, 1880)	Mexico
		Neolycus schönherri (Chevrolat, 1834)	Mexico
		Neolycus scutellatus (Gorham, 1880)	Mexico
		Rhyncheros sp. 1	Mexico
		Rhyncheros sp. 2	Mexico
		Rhyncheros sp. 3	Mexico
		Rhyncheros sp. 4	Mexico
		Rhyncheros carnifex (Gorham, 1880)	Mexico
		Rhyncheros fuliginosus (Gorham, 1880)	Mexico
		Rhyncheros fulvellus (LeConte, 1881)	Mexico and USA
		Rhyncheros fulvellus femoratus (LeConte, 1881)	Mexico
		Rhyncheros godmani (Gorham, 1880)	Mexico
		Rhyncheros lateralis (Melsheimer, 1846)	USA
		Rhyncheros lineicollis (Chevrolat, 1834)	Mexico
		Rhyncheros loripes (Chevrolat, 1834)	Mexico
		Rhyncheros minutus (Green, 1949)	Mexico and USA
		Rhyncheros nigrofumosus (Hinton, 1933)	Mexico
		Rhyncheros rusticus (Gorham, 1884)	Mexico
		Rhyncheros sagittatus (Green, 1949)	Mexico
		Rhyncheros sanguineus (Gorham, 1884)	Mexico
		Rhyncheros sanguinipennis Say, 1823	Mexico
		Rhyncheros semiustus (Chevrolat, 1834)	Mexico
		Rhyncheros simulans (Schaeffer, 1911)	Mexico
		Rhyncheros sordidus Gorham, 1880	Mexico

Table 1 (continued). Taxon sampling, with indication of the country.

Family	Tribe	Species	Country
	Outgroup		
Lycidae	Calopterini	*Calopteron bifasciatum* Gorham, 1884	Mexico
		Calopteron jimenezi Dugés, 1878	Mexico
		Calopteron corrugatum Candeze, 1861	Mexico
		Calopteron discrepans Newman, 1838	Mexico
		Caenia sinuata Kirsch, 1865	Mexico
		Caenia amplicornis LeConte, 1881	USA
Cantharidae		*Chauliognathus* sp.	Mexico

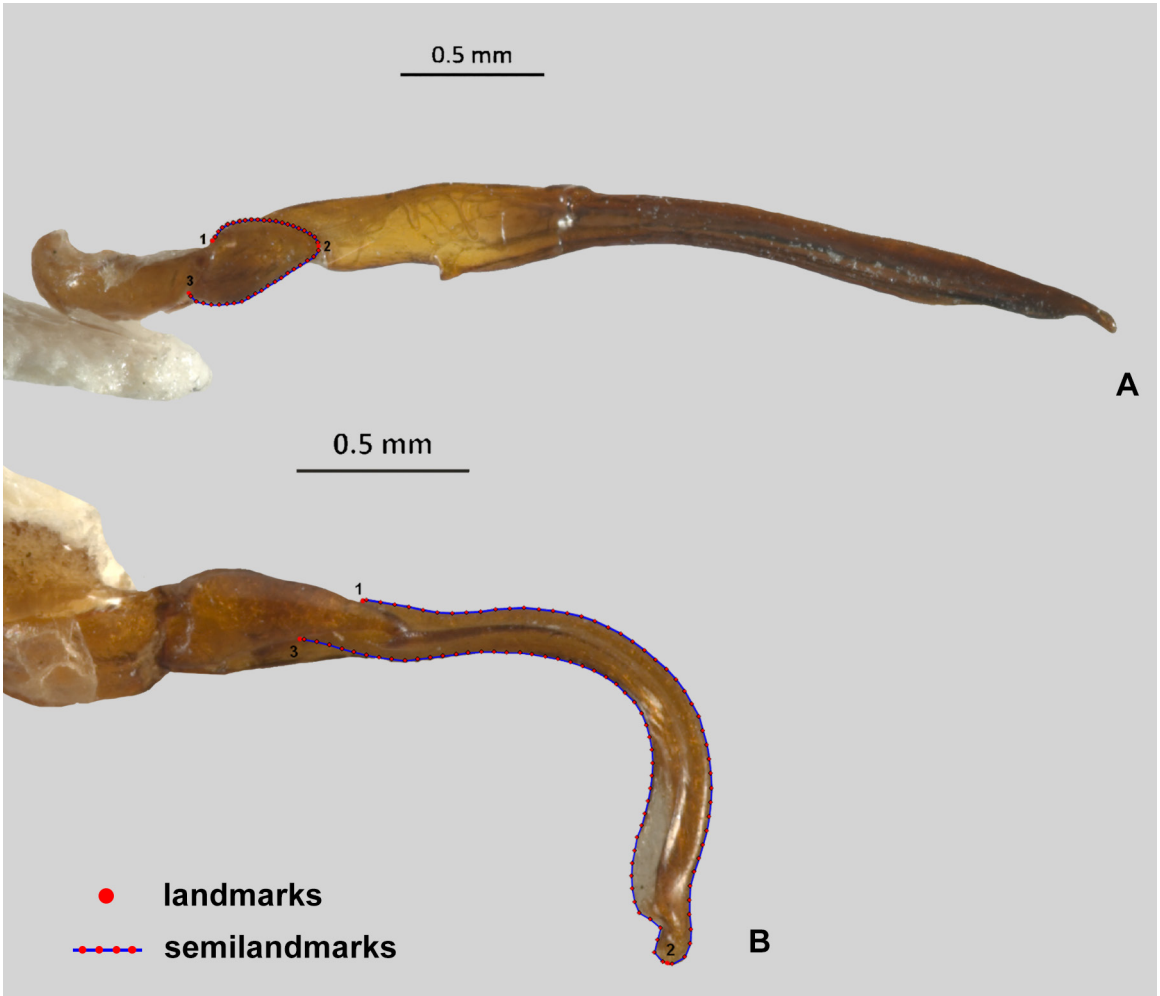

Fig. 1. Designation of landmarks and semilandmarks for the geometric morphometric analysis. **A**. In character 70, three landmarks were selected in the left paramere (one on the right side, one on the apex, and one on the left side), and 40 semilandmarks. **B**. In character 72, three landmarks were selected in the phallus (one on the right, another on the apex, and a third on the left), and 70 semilandmarks.

MRC5 digital camera and Lens Plan NeoFluar, at the Laboratorio de Microscopía y Fotografía de la Biodiversidad at the Instituto de Biología, UNAM (Universidad Nacional Autónoma de México). We registered landmark (LM) and semilandmark (SLM) points with each digital photograph using tpsDig2 ver. 2.3.2 (Rohlf 2017). For character 70, we selected three landmarks on the left paramere: one on the right side, one on the apex, and one on the left side. The landmarks on the right and left sides were situated at the point where the paramere joins the phallobase, and the posterior landmark was placed at the apex of the paramere (3 LM, and 40 SLMs) (Fig. 1A). For character 72, we selected three landmarks on the phallus: one on the right, another on the apex, and a third on the left. The landmarks on both sides were located at the junction between the phallus and the parameres, while the posterior landmark was located at the apex of the phallus (3 LM, and 70 SLMs) (Fig. 1B). All outlines were registered as SLMs using tpsDig2 ver. 2.3.2 (Rohlf 2017), consistently registering equivalent points along outlines 'by length'. To identify the groups with the highest similarity in shape for these structures (character states), we conducted a hierarchical cluster analysis for each structure using an Euclidean distance matrix. The difference matrix obtained was plotted on a dendrogram, which served as a guide for the character state assignment (Figs 2–3, respectively). The optimal number of clusters was determined using the 'elbow' method. All cluster analyses were conducted using RStudio software (R Core Team 2021) with ggplot2 (Wickham 2016) and factoextra (Kassambara & Mundt 2020).

Many characters included in this study were previously used in phylogenetic analyses of the family (Kazantsev 2003, 2013; Bocakova 2005) or for species descriptions (Chevrolat 1834; Gorham 1880; Green 1949; Zaragoza-Caballero 1995; Zaragoza-Caballero & González-Ramírez 2019). Several characters are used here for the first time and are indicated by an asterisk in the character list (see below). A total of 91 characters were derived from the external morphology of adult specimens, 47 of which are scored here for the first time for all included taxa. Twenty characters were obtained from male and female genitalia, 15 of which are reported here for the first time for all included taxa. A total of 31 binary and 60 multistate characters were coded, three characters (4, 27 and 42) were coded as polymorphic for at least some terminals. For continuous characters (1, 28, 41, 42, 52, 77, 80, 84), the designation of character states was carried out in accordance with the formula proposed by Vega-Badillo *et al.* (2021). This entailed calculating the difference between the minimum and maximum values (dmm) and dividing it by the number of character states. The resulting value was then expressed as dmm = max − min / 3. Subsequently, character states were assigned as follows: 0 = min + dmm; 2 = max − dmm; and 1 = intervals between 0 and 2. Individual consistency and retention indices (CI, RI) are provided for all characters from the implied weights analysis (k = 7.187500; see below under Phylogenetic analysis).

Character and character states

Head

0. Coronal sulci: deeply divided (0) (Fig. 4A); slightly divided (1) (CI = 0.50; RI = 0.88).

1. *Width of interantennal distance: less than 0.09 mm (0) (Fig. 4B); 0.1 mm–0.12 mm (1) (Fig. 4C); more than 0.13 mm (2) (Fig. 4D) (CI = 0.40; RI = 0.76).

2. Male IV–X antennomeres shape: bidentate (0) (Fig. 4E); unidentate (1) (Fig. 4F); rectangular (2) (Fig. 4G); filiform (3) (CI = 0.30; RI = 0.58).

3. Female IV–X antennomeres shape: bidentate (0); unidentate (1); rectangular (2); filiform (3) (CI = 0.33; RI = 0.40).

4. *First three antennomeres colour: black (0); yellow (1); bicolour (2) (CI = 0.40; RI = 0.75).

5. Antennomere III proportional length: elongate, almost subequal in length to antennomere IV (0); short, about 0.3 mm shorter than antennomere IV (1); elongate, about 0.7 mm longer than antennomere IV (2) (CI = 0.66; RI = 0.91).

6. Head with rostrum: absent (0); present (1) (CI = 1; RI = 1).

7. *Rostrum relative length: wider than long (0) (Fig. 4H); as long as wide (1) (Fig. 4I); longer than wide (2) (Fig. 4J) (CI = 0.40; RI = 0.50).

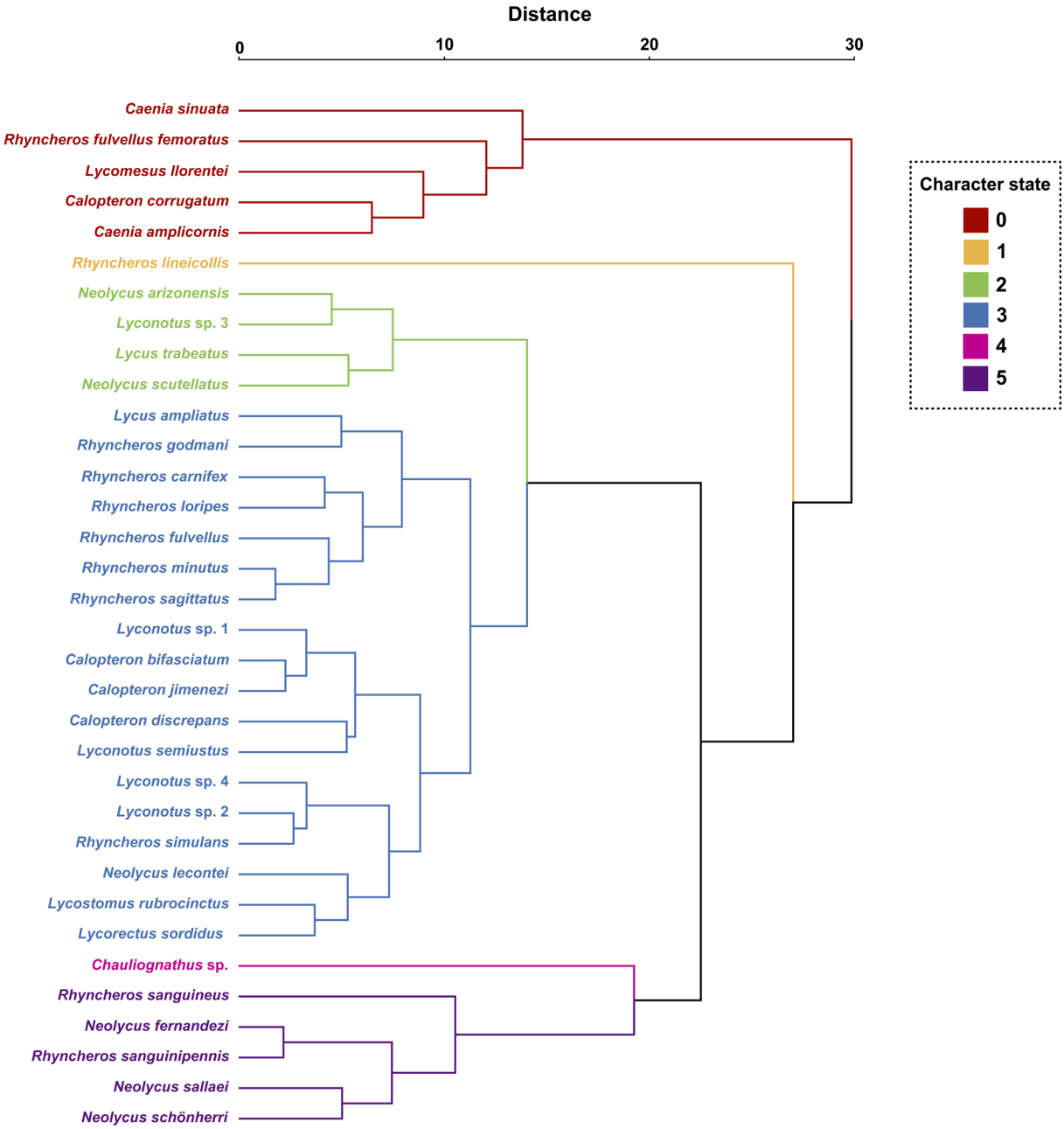

Fig. 2. Dendrogram obtained after digitizing the paramere contour using Euclidian distances, showing the six recognized characters states (character 70).

8. *Rostrum length-width ratio: less than 1.9 (0); 2 to 2.6 (1); more than 2.7 (2) (CI = 0.22; RI = 0.22).

9. *Labrum shape in dorsal view: oval (0) (Fig. 4K); semi-circular (1); semi-square (2) (Fig. 4L); rectangular (3) (Fig. 4M); obcordate (4); bilobate (5) (CI = 0.50; RI = 0.70).

10. *Labrum width-length relation: as wide as long (0); wider than long (1); longer than wide (2) (CI = 0.14; RI = 0.45).

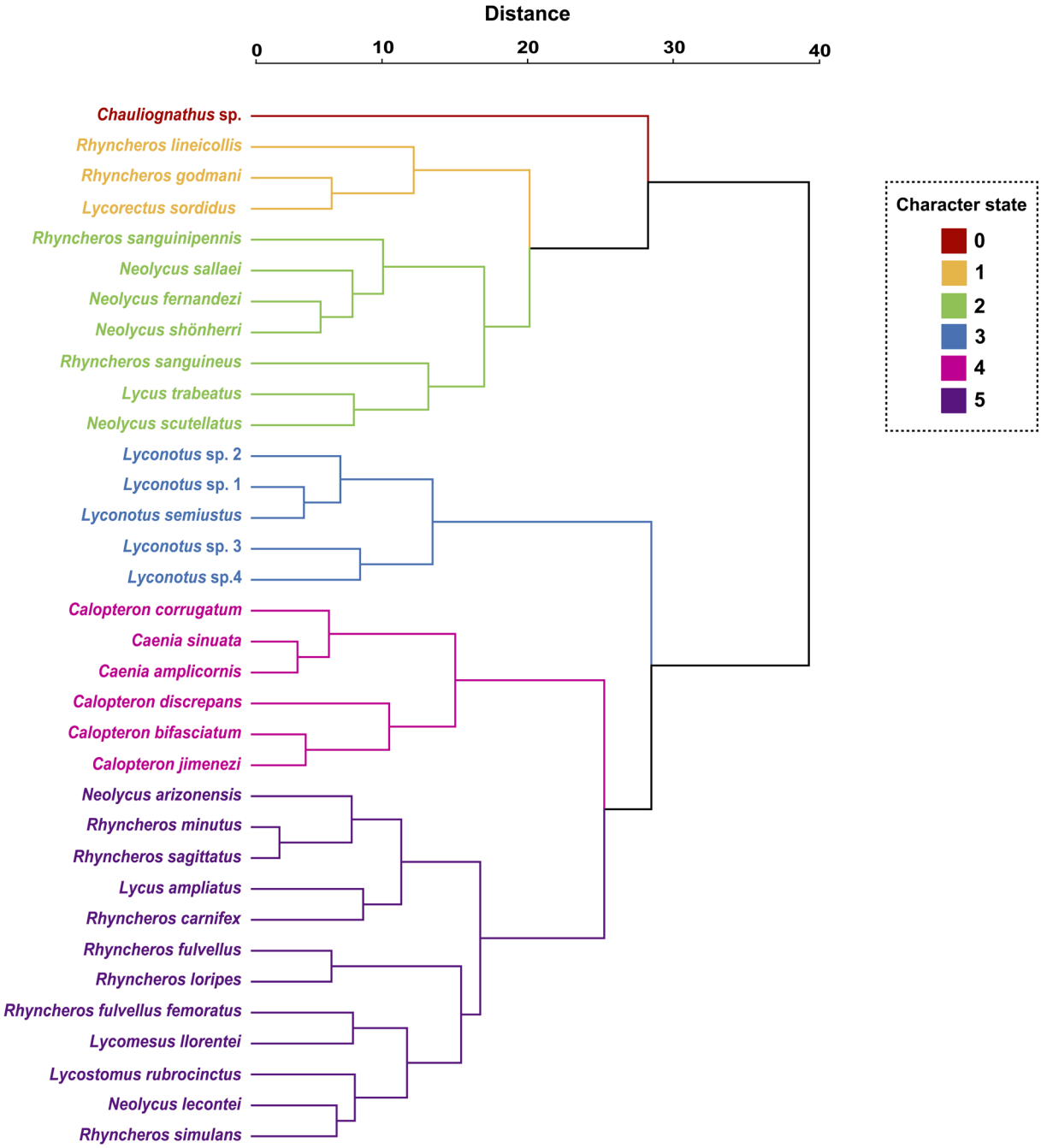

Fig. 3. Dendrogram obtained after digitizing the phallus contour using Euclidian distances, showing the six recognized characters states (character 72).

Fig. 4. Morphology of Lycini. **A**. Frontal hump of *Lyconotus* sp. 2, ♂ (CNIN, QR 70966). **B–D**. Interantennal distance. **B**. *Neolycus fernandezi* (Dugès, 1878), ♂ (CNIN, QR 67699). **C**. *Lyconotus* sp. 1, ♂ (CNIN, QR 70971). **D**. *Rhyncheros minutus* (Green, 1949), ♀ (CNIN, QR 68274). **E–G**. Antenna. **E**. *Neolycus scutellatus* (Gorham, 1880), ♂ (CNIN, QR 67865). **F**. *Neolycus fernandezi*, ♂ (CNIN, QR 67714). **G**. *Lyconotus semiustus* (Chevrolat, 1834), ♂ (CNIN, QR 68724). **H–J**. Rostrum. **H**. *Rhyncheros carnifex* (Gorham, 1880), ♀ (CNIN, QR 67878). **I**. *Rhyncheros lineicollis* (Chevrolat, 1834), ♂ (CNIN, QR 67905). **J**. *Rhyncheros loripes* (Chevrolat, 1834), ♀ (CNIN, QR 68185). **K–M**. Labrum. **K**. *Lyconotus* sp. 3, ♀ (CNIN, QR 70975). **L**. *Rhyncheros minutus*, ♂ (CNIN, QR 68294). **M**. *Neolycus scutellatus*, ♂ (CNIN, QR 67856). **N–P**. Maxillary palpomere. **N**. *Neolycus schoenherri* (Chevrolat, 1834), ♂ (CNIN, QR 67841). **O**. *Lycostomus rubrocinctus* Fairmaire, 1886, ♂ (CNIN, China). **P**. *Neolycus arizonensis* (Green, 1949), ♂ (CNIN, QR 67730). **Q–X**. Pronotum. **Q**. *Lycostomus rubrocinctus*, ♂ (CNIN, China). **R**. *Neolycus arizonensis*, ♂ (CNIN, QR 67734). **S**. *Neolycus schoenherri*, ♂ (CNIN, QR 67820). **T**. *Rhyncheros loripes*, ♂ (CNIN, QR 68093). **U**. *Rhyncheros lineicollis*, ♂ (CNIN, QR 67913). **V**. *Lyconotus* sp. 2, ♂ (CNIN, QR 70966). **W**. *Rhyncheros fuliginosus* (Gorham, 1880), ♂ (CNIN, QR 67757). **X**. *Lyconotus* sp. 4, ♂ (CNIN, QR 70967).

11. *Labrum anterior margin shape: straight (0); rounded (1); emarginate (2); bilobate (3); cleft (4); truncated (5) (CI = 0.50; RI = 0.75).

12. *Labrum lateral margins shape: straight (0); semi-rounded (1); rounded (2) (CI = 0.16; RI = 0.54).

13. Shape of the mandible: straight (0); curved (1) (CI = 1; RI = 1).

14. *Mandible relative length: shorter than labrum (0); as long as labrum (1); longer than labrum (2) (CI = 0.66; RI = 0.93).

15. Shape of the last maxillary palpomere: fusiform (0); rectangular (1) (Fig. 4N); securiform (2) (Fig. 4O); sub-securiform (3) (Fig. 4P) (CI = 0.33; RI = 0.60).

16. *Fourth maxillary palpomere dilated at the apex: absent (0); present (1) (CI = 0.14; RI = 57).

17. *Fourth maxillary palpomere relative length: shorter than second (0); as long as second (1); longer than second (2) (CI = 0.18; RI = 0.52).

18. Last labial palpomere shape: rectangular (0); transversely triangular (1); securiform (2) (CI = 0.28; RI = 0.61).

19. *Length of the palpifer relative to the prementum: 2× longer (0), 1× longer (half the length of palpifer) (1); as long as prementum (2); 0.5× longer (3) (CI = 0.33; RI = 0.73).

20. *Appearance of the prementum: slender (0); robust (1) (CI = 0.33; RI = 0.83).

21. Prementum with a median suture: absent (0); present (1) (CI = 0.07 RI = 0.29).

Thorax

22. Pronotum anterior margin shape: rounded (0) (Fig. 4Q); angulated (1) (Fig. 4R); obtuse (2) (CI = 0.28; RI = 0.37).

23. Length of the anterior angles of the male pronotum: short (0) (Fig. 4S); approximately half the length of the anterior margin of pronotum (1) (Fig. 4T); as long as the anterior margin of pronotum (2) (Fig. 4U) (CI = 0.50; RI = 0.60).

24. Female pronotum anterior angles: short (0); approximately half the length of the anterior margin of pronotum (1) (CI = 0.50; RI = 0).

25. Pronotum lateral margins shape: nearly straight (0) (Fig. 4V); rounded (1) (Fig. 4W) (CI = 0.14; RI = 0.66).

26. *Surface texture of the pronotal lateral margins: punctuated (0); roughly punctuated (1) (CI = 0.25; RI = 0.66).

27. *Pronotal pubescence density on lateral margins: scarce (0); moderate (1); abundant (2) (CI = 0.25; RI = 0.73).

28. *Pronotal margin width: less than 0.52 mm (0) (Fig. 4X); 0.53 mm–0.81 mm (1) (Fig. 5A); more than 0.82 mm (2) (Fig. 5B) (CI = 0.22; RI = 0.61).

29. *Pronotum median black spot: absent (0); present (1) (CI = 0.20; RI = 0.63).

30. *Pronotum median black spot size: wide, occupying half of pronotal disc (0); wide, occupying nearly all pronotal disc (1); narrow, triangular (2); narrow, as a longitudinal line (3); narrow, as two longitudinal lines (4) (CI = 0.30; RI = 0.30).

31. Pronotum with a median longitudinal carina: absent (0); complete (1); incomplete, present only anteriorly (2); incomplete, present anteriorly or posteriorly (3) (CI = 0.42; RI = 0.55).

32. *Pronotum longitudinal areola width: narrow, limited to a straight line (0); wide, thin spindle-shaped (1); wide, spindle-shaped (wide in the middle) (2); spindle-like thin at the apex and broad at the base (3) (CI = 0.27; RI = 0.38).

33. *Pronotal disc pubescence density: scarce (0); moderate (1); abundant (2) (CI = 0.28; RI = 0.75).

34. Prosternum presentation: not protuberant (0); protuberant (1) (CI = 0.12; RI = 0.53).

35. Prosternum carination: absent (0); present (1) (CI = 0.16; RI = 0.72).

36. Prosternum carination presentation: slightly visible (0); strongly visible (1) (CI = 0.16; RI = 0.44).

37. *Cervical sclerites shape: semicircular (0) (Fig. 5C); fusiform (1) (Fig. 5D); elongate (2); triangular (3) (CI = 0.42; RI = 0.71).

38. *Prosternum posterior border shape: rounded (0); truncated (1) (CI = 0.10; RI = 0.47).

39. *Sternellum shape: transverse (0); transverse with posterior branches (1); inverted ‘V’ with short branches (2); inverted ‘V’ with long branches (3) (CI = 0.21; RI = 0.21).

40. Elytra dilated position: on the humeral region (0); on the middle (1) (Fig. 5E); towards apex (2) (Fig. 5F) (CI = 0.33; RI = 0.42).

41. *Male elytra dilated width-humeral width ratio: less than 1.79 (0); 1.8 to 2.9 (1); more than 3 (2) (Fig. 5G) (CI = 0.22; RI = 0.63).

42. *Female elytra dilated width-humeral width ratio: less than 1.66 (0) (Fig. 5H); 1.7 to 2.1 (1) (Fig. 5I); more than 2 (2) (CI = 0.40; RI = 0.62).

43. Elytra coloration: unicolorous (0); bicolored (1) (CI = 0.50; RI = 0.90).

44. *Elytra apex shape: blunt (0) (Fig. 5J); rounded (1) (Fig. 5K); acute (2) (Fig. 5H) (CI = 0.40; RI = 0.75).

45. *Colour of the scutellum: yellow (0); black (1); red (2) (CI = 0.28; RI = 0.50).

46. Scutellum shape: quadrangular (0); spatula-shape (1); triangular (2) (CI = 0.22; RI = 0.56).

47. Width-length relation of the scutellum: as wide as long (0); wider than long (1); longer than wide (2) (CI = 0.22; RI = 0.30).

48. Shape of scutellum apex: truncated (0); rounded (1); emarginated (2); bipartite (3); acute (4) (CI = 0.50; RI = 0.66).

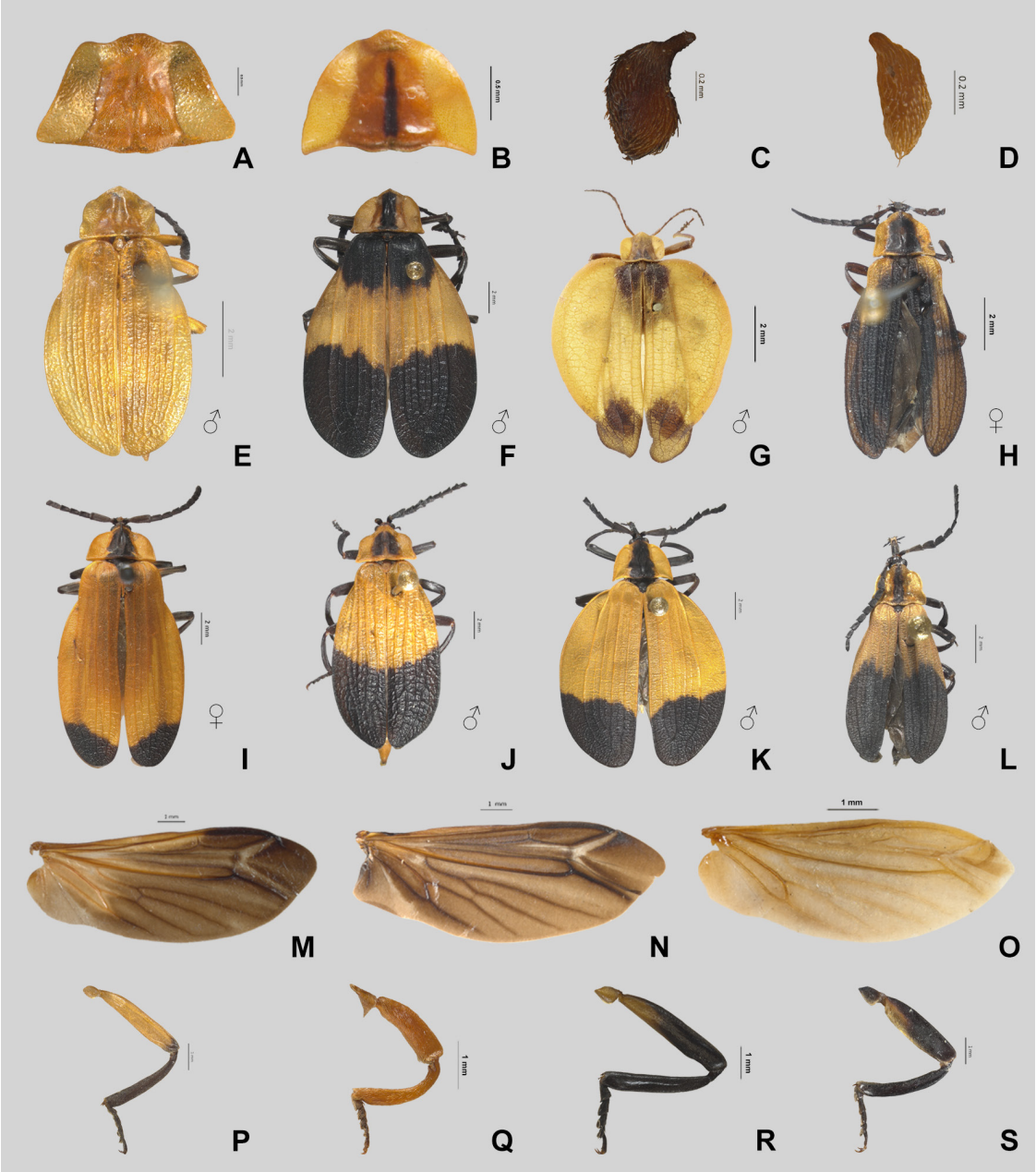

Fig. 5. Morphology of Lycini. **A–B**. Pronotum. **A**. *Rhyncheros sagittatus* (Green, 1949), ♂ (CNIN, QR 68333). **B**. *Rhyncheros fulvellus femoratus* (Schaeffer, 1911), ♂ (CNIN, QR 68361). **C–D**. Cervical sclerites. **C**. *Neolycus fernandezi* (Dugès, 1878), ♂ (CNIN, QR 67753). **D**. *Lyconotus* sp. 3, ♂ (CNIN, QR 70965). **E–G**. Male elytra. **E**. *Rhyncheros loripes* (Chevrolat, 1834), ♂ (CNIN, QR 68036). **F**. *Neolycus sallaei* (Gorham, 1880), ♂ (CNIN, QR 67788). **G**. *Lycus trabeatus* Guérin-Méneville, 1835, ♂ (NHMUK 015010150) (Photo: Keita Matsumoto). **H–I**. Female elytra. **H**. *Lyconotus lateralis* (Green, 1949), ♀ (CNIN, QR 67895). **I**. *Neolycus fernandezi*, ♀ (CNIN, QR 67717). **J–L**. Elytra apex. **J**. *Neolycus scutellatus* (Gorham, 1880), ♂ (CNIN, QR 67864). **K**. *Neolycus schoenherri* (Chevrolat, 1834), ♂ (CNIN, QR 67846). **L**. *Lyconotus semiustus* (Chevrolat, 1834), ♂ (CNIN, QR 68441). **M–O**. Wing: **M**. *Neolycus lecontei* (Green, 1949), ♂ (CNIN, QR 67897). **N**. *Rhyncheros sanguinipennis* Say, 1823, (CNIN, Mexico). **O**. *Lyconotus* sp. 4, ♂ (CNIN, QR 70967). **P–S**. Metaleg. **P**. *Neolycus arizonensis* (Green, 1949), ♂ (CNIN, QR 67738). **Q**. *Lyconotus* sp. 1, ♂ (CNIN, QR 70971). **R**. *Neolycus sallaei*, ♂ (CNIN, QR 67780). **S**. *Neolycus scutellatus*, ♂ (CNIN, QR 67861).

49. *Shape of radio medial loop: elliptical (0) (Fig. 5M); rounded (1) (Fig. 5N); acute (2) (Fig. 5O); acuminate (3); sharp edges (4) (CI = 0.80; RI = 0.93).

50. Mesosternum protuberance: not protuberant (0); slightly protuberant (1); strongly protuberant (2) (CI = 0.28; RI = 0.70).

51. Mesosternum shape: wide (0); divided in two sclerites (1); narrow (2) (CI = 0.33; RI = 0.69).

52. *Relative size of furca: less than 0.17 mm (0); 0.18 mm–0.26 mm (1); more than 0.27 mm (2) (CI = 0.28; RI = 0).

53. Shape of inner angle of male metacoxae: blunt (0); rounded (1); acute (2) (CI = 0.18; RI = 0.59).

54. Shape of inner angle of female metacoxae: blunt (0); rounded (1); acute (2) (CI = 0.22; RI = 0.50).

55. Spinose male trochanters: absent (0) (Fig. 5P); present (1) (Fig. 5Q) (CI = 1; RI = 1).

56. Spinose female trochanters: absent (0); present (1) (CI = 1; RI = 1).

57. Relative size of male metafemora: not robust (0) (Fig. 5R); robust (1) (Fig. 5S) (CI = 0.11; RI = 0.50).

58. Relative size of female metafemora: not robust (0); robust (1) (CI = 0.14; RI = 0.14).

59. Shape of male metatibiae: straight (0) (Fig. 6A); arcuate (1) (Fig. 6B); sickle-shaped (2) (Fig. 6C) (CI = 0.28; RI = 0.75).

60. Shape of female metatibiae: straight (0); arcuate (1) (CI = 0.33; RI = 0.75).

61. Appearance of metatibial spurs: similar (both acute) (0) (Fig. 6D); dissimilar (inner acute, outer slightly broader apically and bluntly rounded) (1) (Fig. 6E) (CI = 1; RI =1).

62. *Relative length of metatibial spurs: short (0) (Fig. 6F); long (1) (Fig. 6G) (CI = 1; RI = 1).

Abdomen

63. *Shape of posterior border of sixth sternite in males: straight (0) (Fig. 6H); concave (1) (Fig. 6I); deeply concave (2) (Fig. 6J); cleft (3) (Fig. 6K); emarginate (4); convex (5) (Fig. 6L) (CI = 0.35; RI = 0.43).

64. *Shape of posterior border of sixth sternite in females: straight (0) (Fig. 6M); wavy (1); concave (2) (Fig. 6N); emarginate (3); cleft (4) (CI = 0.66; RI = 0.75).

65. Last sternite medially curved in males: absent (0) (Fig. 6O); present (1) (Fig. 6P) (CI = 1; RI = 1).

66. *Shape of posterior border of last sternite in females: rounded (0); emarginate (1) (Fig. 6Q); cleft (2) (Fig. 6R); horseshoe-shaped (3) (Fig. 6S); auricle shaped (4) (CI = 0.40; RI = 62).

67. *Shape of apex of the last sternite in females: rounded (0); acute (1); acuminate (2); straight (3); undifferentiated (4) (CI = 0.44; RI = 50).

Fig. 6. Morphology of Lycini. **A–C**. Metaleg. **A**. *Rhyncheros godmani* (Gorham, 1880), ♂ (CNIN, QR 67894). **B**. *Neolycus schoenherri* (Chevrolat, 1834), ♂ (CNIN, QR 67836). **C**. *Lyconotus semiustus* (Chevrolat, 1834), ♂ (CNIN, QR 70971). **D–G**. Metatibial spurs. **D**. *Rhyncheros sanguinipennis* Say, 1823, ♂ (CNIN, Mexico). **E**. *Neolycus fernandezi* (Dugès, 1878), ♂ (CNIN, QR 67754). **F**. *Lyconotus* sp. 4, ♂ (CNIN, QR 70967). **G**. *Rhyncheros minutus* (Green, 1949), ♂ (CNIN, QR 68270). **H–L**. Male abdomen. **H**. *Rhyncheros fulvellus* (LeConte, 1881), ♂ (CNIN, 67915). **I**. *Rhyncheros simulans* (Schaeffer, 1911), ♂ (CNIN, QR 68418). **J**. *Lyconotus semiustus*, ♂ (CNIN, QR 68724). **K**. *Neolycus arizonensis* (Green, 1949), ♂ (CNIN, QR 67744). **L**. *Lycorectus sordidus* (Gorham, 1880) gen. et comb. nov., ♂ (CNIN, QR 68429). **M–N**. Female abdomen. **M**. *Neolycus sallaei* (Gorham, 1880), ♀ (CNIN, QR 67771). **N**. *Lyconotus semiustus*, ♀ (CNIN, QR 68730). **O–P**. Lateral view of male abdomen. **O**. *Rhyncheros sanguinipennis*, ♂ (CNIN, Mexico). **P**. *Lyconotus semiustus*, ♂ (CNIN, QR 68737). **Q–S**. Female abdomen. **Q**. *Rhyncheros minutus*, ♀ (CNIN, QR 68259). **R**. *Rhyncheros sanguineus* (Gorham, 1884), ♀ (CNIN, Mexico). **S**. *Lycostomus praeustus* Fabricius, 1792, ♀ (CNIN, QR 68440). **T**. Male genitalia; *Neolycus lecontei* (Green, 1949), ♂ (CNIN, QR 67901).

Male genitalia

68. Length relation between phallobase (= basal piece) and parameres (= lateral lobes): phallobase as long as parameres (0) (Fig. 6T); longer (1) (Fig. 7A); shorter (2) (Fig. 7B) (CI = 0.33; RI = 0.76).

69. Parameres apex: partially fused with phallus (0) (Fig. 7C); free but attached to phallus (1) (Fig. 7D); free (2) (CI = 0.50; RI = 0.33).

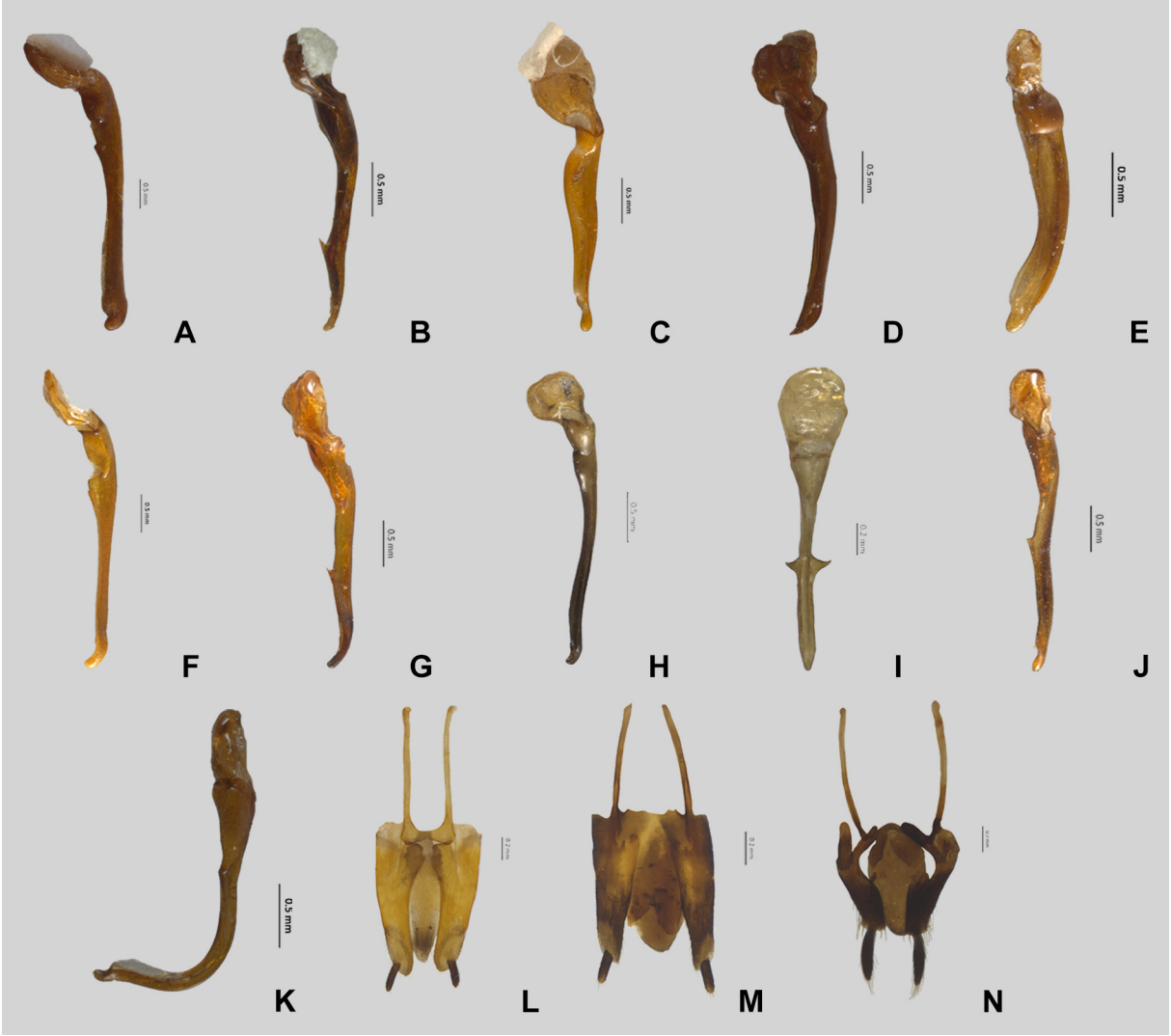

Fig. 7. Morphology of Lycini. **A–K**. Male genitalia. **A**. *Neolycus scutellatus* (Gorham), ♂ (CNIN, QR 67864). **B**. *Neolycus arizonensis* (Green, 1949), ♂ (CNIN, QR 67750). **C**. *Rhyncheros loripes* (Chevrolat, 1834), ♂ (CNIN, QR 68024). **D**. *Lycus ampliatus* (Fåhraeus, 1851), ♂ (CNIN, QR 68420). **E**. *Lycomesus llorentei* Zaragoza-Caballero & González-Ramírez, 2019, ♂ (CNIN, QR 70969). **F**. *Rhyncheros sanguineus* (Gorham, 1884), ♂ (CNIN, QR 38355). **G**. *Neolycus sallaei* (Gorham, 1880), ♂ (CNIN, QR 67781). **H**. *Rhyncheros nigrofumosus* (Hinton, 1933), ♂ (CNIN, QR 68295). **I**. *Rhyncheros sagittatus* (Green, 1949), ♂ (CNIN, QR 68302). **J**. *Neolycus schoenherri* (Chevrolat, 1834), ♂ (CNIN, QR 67837). **K**. *Lyconotus semiustus* (Chevrolat, 1834), ♂ (CNIN, QR 70970). **L–N** Female genitalia. **L**. *Neolycus fernandezi* (Dugès, 1878), ♀ (CNIN, QR 67673). **M**. *Rhyncheros carnifex* (Gorham, 1880), ♀ (CNIN, QR 67878). **N**. *Lyconotus semiustus*, ♀ (CNIN, QR 67674).

70. *Parameres shape in lateral view was assigned to a group through of geometrical morphometric analysis (Fig. 2): group 0 (0); group 1 (1); group 2 (2); group 3 (3); group 4 (4); group 5 (5) (CI = 0.38; RI = 0.27).

71. Parameres apex shape: rounded (0) (Fig. 7E); acute (1) (Fig. 7F); acuminate (2) (Fig. 7G) (CI = 0.18; RI = 0.52).

72. *Phallus shape in lateral view was assigned to a group through of geometrical morphometric analysis (Fig. 3): group 0 (0); group 1 (1); group 2 (2); group 3 (3); group 4 (4); group 5 (5) (CI = 0.50; RI =0.70).

73. Pair of thorns on phallus: absent (0) (Fig. 7H); present (1) (Fig. 7I) (CI = 0.25; RI = 0.76).

74. *Phallus thorns location: in ventral view (0) (Fig. 7J); in lateral view (1) (Fig. 7K) (CI = 0.50; RI = 0.83).

75. *Phallus thorns relative position: near parameres (0); around phallus mid-length (1) (CI = 0.33; RI = 0.71).

76. *Phallus thorns modified to receive parameres: absent (0); present (1) (CI = 1; RI = 1).

77. *Phallus thorns relative length: less than 0.046 mm (0); 0.047 mm–0.083 mm (1); more than 0.084 mm (2). (CI = 0.28 RI = 0.16).

78. *Phallus thorns apex shape: truncated (0); rounded (1); acute (2); acuminate (3). (CI = 0.50; RI = 0.66).

79. *Phallus apex shape: rounded (0); sharp (1); bifurcated (2); pincer (3) (CI = 1; RI = 1).

Female genitalia

80. *Stylus length: less than 0.21 mm (0); 0.22 mm–0.29 mm (1); more than 0.30 mm (2) (CI = 0.25; RI = 0.40).

81. *Stylus shape: robust (0); slender (1) (CI = 0.11; RI = 0.20).

82. *Outer margin of the stylus cleft: absent (0); present (1) (CI = 1; RI = 1).

83. *Coxites-valvifers integration: non-joined and separated (0) (Fig. 7L); joined (1); merged (2) (Fig. 7M); non-joined and overlapping structures (3) (Fig. 7N) (CI = 0.75; RI = 0.94).

84. *Coxites length: less than 0.97 mm (0); 0.98 mm–1.50 mm (1); more than 1.51 mm (2) (CI = 0.33; RI = 0.55).

85. Coxites shape: almost straight (0); emarginate medially (1); emarginate apically, S-shaped (2) (CI = 0.22; RI = 0.46).

86. *Outer margin of the coxites cleft: absent (0); present (1) (CI = 1; RI = 1).

87. *Coxites inner apical margins relative position: nearby (0); distant (1) (CI = 0.33; RI = 0.81).

88. *Length relation between coxites and valvifers: shorter (0); coxites as long as valvifers (1); longer (2) (CI = 50; RI = 0.85).

89. Fusion of valvifers at the base: absent (0); present (1) (CI = 0.50; RI = 0.90).

90. *Coxites inner margin base shape: concave (0); lobed (1) (CI = 1; RI = 1).

Phylogenetic analysis

The matrix was created using Winclada ver. 1.00.08 (Nixon 2002). Multistate characters were treated as non-additive. Unknown character states were coded with question marks ('?'), which was mostly the case when only one sex was examined due to the lack of specimens for the other sex; inapplicable character states were coded using a dash ('-') when the preceding character in the matrix was coded as absent. Total polymorphism (all possible character states present in the same taxon) is represented by WinClada using an asterisk ('*'); partial polymorphisms (only some of the possible character states present in the same taxon) are represented by WinClada using dollar symbols ('$').

Phylogenetic analyses were carried out using parsimony, maximum likelihood (ML), and Bayesian inference (BI). Parsimony analyses were conducted using TNT ver. 1.6 (Goloboff & Morales 2023) under equal weights (EW) and heuristic searches used the ratchet method (Nixon 1999). The specific parameters used were: 1000 random seeds, find minimum length at least 10 times, and 5000 iterations. The analysis was conducted on multiple occasions until we established that the results were stable. Winclada ver. 1.00.08 (Nixon 2002) was used to construct a strict consensus tree (Nixon & Carpenter 1996) from the most parsimonious trees. These trees were evaluated by tree length (L), consistency index (CI), and retention index (RI). To examine the effect of individual character homoplasy on the analyses results, we conducted a second analysis using implied weights (IW; Goloboff 1993). We used the TNT script (setk.run) written by Salvador Arias (Hermes *et al.* 2014) to determine the optimal value for the constant *k* (Goloboff *et al.* 2008). A value of 7.187500 was returned as the most appropriate *k* value and was therefore used in all subsequent implied weighting schemes employing the heuristic method of new search strategies (ratchet), with the following parameters: 1000 random seeds, find minimum length 10 times and 5000 iterations. The optimal trees were opened in Winclada ver. 1.00.08 (Nixon 2002) to calculate the length and consistency and retention indices as well as to construct their strict consensus tree (Nixon & Carpenter 1996). To assess the statistical branch support, a bootstrap (BS) and a jackknife (JS) analyses were carried out with NONA (Goloboff 1994) through WinClada ver. 1.00.08 (Nixon 2002). Ten thousand replicates were conducted utilizing 10 initial trees, holding 10 trees and expanding the memory up to 1000 trees (mult*10 hold/10 max*10 000). We considered strong support above 80%. The character optimizations were mapped on the strict consensus tree in Winclada ver. 1.00.08 (Nixon 2002). Three different optimizations were employed: unambiguous changes, and accelerated (ACCTRAN) and delayed (DELTRAN) transformations (Supp. file 4: figs S1–S3). The decision to employ DELTRAN was motivated by the fact that, in certain instances, when there are terminals with unknown or inapplicable states, ACCTRAN considers it to be a spurious synapomorphy. In contrast, DELTRAN does not execute this transformation, considering an apomorphy exclusively for taxa that possess the given state (De Santis & Nihei 2022). The presence of artefacts in the mapping process was investigated through a thorough examination of polytomies. This involved a meticulous comparison of the location of character states among the most parsimonious or optimal trees in branches supporting polytomies. Toggling the options to map characters vs character states was used to verify the distribution of character states among our taxon sample for identifying diagnostic characters.

IQ-Tree 2 software (Minh *et al.* 2020) was used for maximum likelihood inference (ML). The evolutionary model was obtained using ModelFinder (Kalyaanamoorthy *et al.* 2017) implemented in IQ-Tree 2. According to the Bayesian information criterion (BIC), the best fit model was the k-states Markov Mkv (MK) (Lewis 2001) with verification bias correction (ASC), gamma distribution using four categories of discrete rates (G4), and equal state frequencies (FQ). Branch support was estimated by ultrafast bootstrapping (UFBoot) using 10 000 replicates (Hoang *et al.* 2018). Values ≥ 95% were considered indicative of strong support.

Bayesian inference (BI) was performed using Mr. Bayes ver. 3.2.7 (Ronquist *et al.* 2012), using the Mkv model (Ronquist & Huelsenbeck 2003) for variable morphological characters, with gamma for state frequencies and 0.07 for temperature. Four simultaneous runs of two million generations were run, each with one cold chain and three heated chains. Samples were drawn every 500 Markov chain Monte Carlo steps, with the first 25% discarded as burn-in. The run was automatically stopped when the average standard deviation of split frequencies was below 0.01. The posterior probability (PP) was employed to provide support for the nodes (Yang & Rannala 1997), values ≥95% were interpreted as high nodal support and ≥80% for standard BS values. Phylogenetic trees were visualized in FigTree ver. 1.4.4 (Rambaut 2009).

The four phylogenetic hypotheses were subjected to statistical analysis to determine their statistical significance (p-value of 0.05). To this end, the following parsimony-based tree topology tests were conducted: Templeton test and winning-sites test, implemented in PAUP ver. 4.0a software (Swofford & Bell 2017), and likelihood-based tests: the weighted Kishino-Hasegawa (KH) test, the weighted Shimodaira-Hasegawa (SH) test and Shimodaira's approximately unbiased (AU) test with IQ-Tree 2 software (Minh *et al.* 2020).

Results

Phylogenetic analysis

Input data

The data matrix comprises 219 cells coded as missing (?), 176 as not applicable (-), five as full polymorphisms, and 23 as partial polymorphisms. The complete matrix used for the morphological analysis can be found in Supp. file 2: table 1. The application of different approaches yielded congruent patterns on major linages.

Parsimony analysis using equal weights

The parsimony analysis under EW yielded 4 most parsimonious trees, with a length of 581 steps, a consistency index (CI) of 0.32, and a retention index (RI) of 0.63. The strict consensus tree has 587 steps (CI = 0.31; RI = 0.63) (Supp. file 3: fig. S1). The tribe Lycini was recovered as monophyletic (BS = 70; JS = 79), but *Lycostomus*, *Rhyncheros* and *Neolycus* were not recovered as monophyletic. However, three clades within the tribe were recovered as monophyletic: *Lycus*, *Lycomesus*, and *Lyconotus* (BS = 85; JS = 89) (Supp. file 3: fig. S1).

Parsimony analysis using implied weights

The parsimony analyses under IW with a constant $k = 7.187500$ using the TNT script (setk.run) resulted in one most parsimonious tree (L = 583, CI = 0.31, RI = 0.63) (Supp. file 4: fig. S2). Bootstrap and jackknife values for each branch are shown in Fig. 8. As is common with morphological matrices, most clades received low support (Bocakova 2001, 2005; Nascimento *et al.* 2020; Vega-Badillo *et al.* 2021). The cladogram under IW shows that the Lycini are monophyletic (BS = 69; JS = 80), and their sister group is *Caenia* + *Calopteron* (Fig. 8). The monospecific genus *Lycomesus* was recovered as the sister group to *Lyconotus* (Fig. 8), and *Lyconotus* was recovered as monophyletic (BS = 84; JS = 88). However, *Lycostomus* was not found to be monophyletic (Fig. 8). *Lycus* was recovered as sister to the remaining North American Lycini (Fig. 8). *Lycorectus sordidus* (Gorham, 1880) gen. et comb. nov. was recovered as sister to *Neolycus* and the rest of *Rhyncheros* (Fig. 8). The analysis shows that *Neolycus* was monophyletic (BS = 59; JS = 64). Fourteen species of *Rhyncheros* were forming a clade (Fig. 8).

Maximum likelihood analysis

The ML analysis yielded a topology that was well resolved, exhibiting a high degree of congruence with the topology obtained under IW (Supp. file 5: fig. S1). The monophyly of the Lycini was recovered with

strong nodal support (UFBoot = 99%). The analysis revealed that the clade *Lycomesus* + *Lyconotus* was a sister group to all Lycini. *Lycostomus* was recovered as non-monophyletic. The monophyly of *Lyconotus* and *Lycus* was well supported with 96% and 91% of UFBoot, respectively. The analysis further revealed *Rhyncheros* to be paraphyletic, *Lycorectus sordidus* gen. et comb. nov. was recovered as sister group to *Neolycus*, and the monophyly of *Neolycus* was supported by a low UFBoot value (80%) (Supp. file 5: fig. S1).

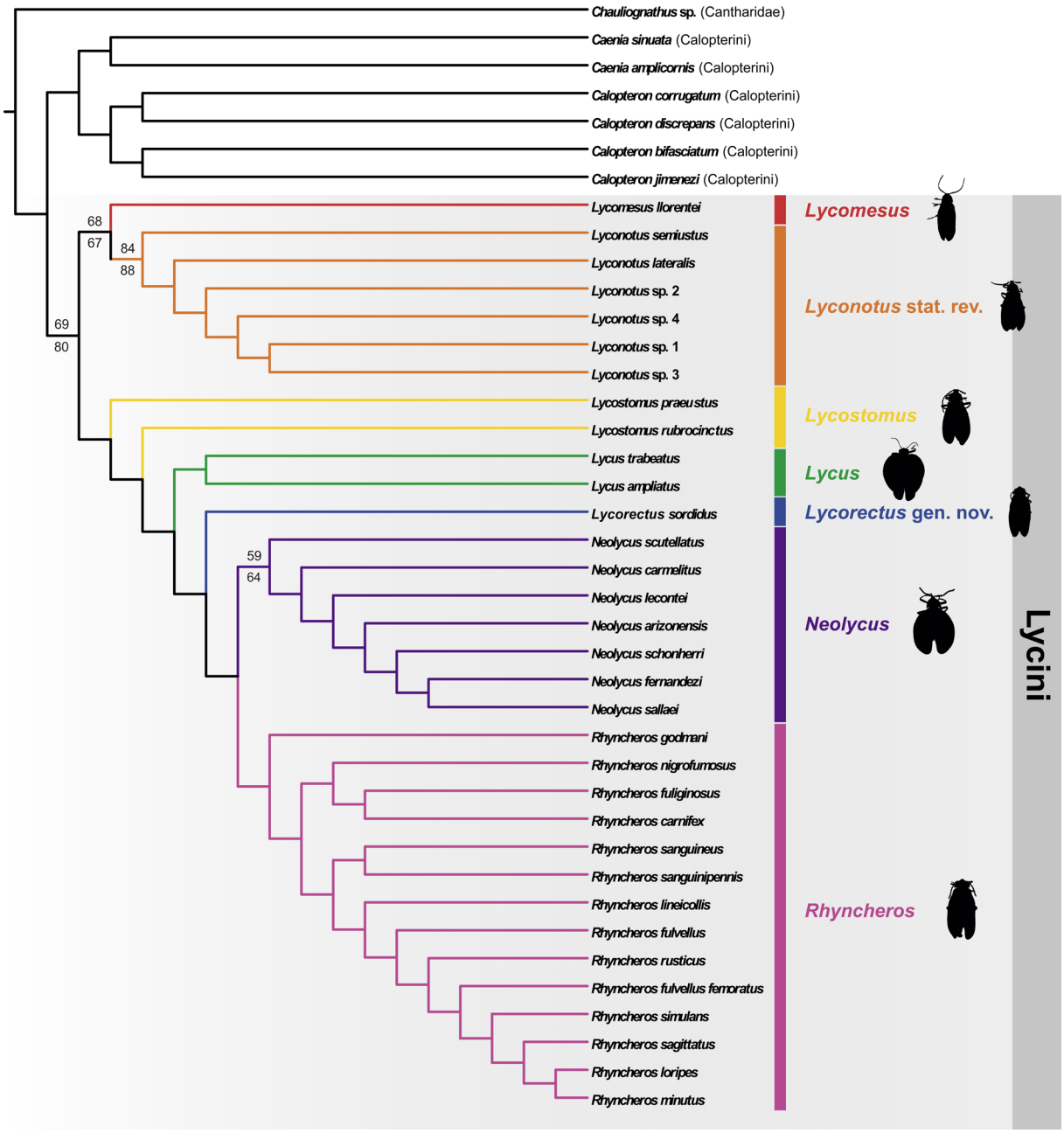

Fig. 8. A single cladogram of parsimony analysis under implied weights (L = 583 CI = 0.31; RI = 0.63). above branches indicate bootstrap values and numbers below the branches corresponds to the jackknife values (> 50).

Table 2. Results of tree topology tests. P-EW signifies parsimony under equal weights, whilst P-IW denotes parsimony under implicated weights, ML indicates maximum likelihood, and BI indicates Bayesian inference for each topology. Parsimony-based tests: Templeton and winning-sites were performed on the PAUP ver. 4.0a software (Swofford & Bell 2017). Likelihood-based topology tests: weighted Kishino-Hasegawa test (W-KH), weighted Shimodaira-Hasegawa test (W-SH), and Shimodaira's approximately unbiased test (AU) were performed on IQ-Tree 2 software (Minh *et al*. 2020). Grey color denotes p-value > 0.05 (statical significance). 'best' means that the tree was the best tree for a given optimality criterion.

Topology	Templeton	winning-sites	W-KH	W-SH	AU
P-EW	0.627	0.486	0.233	0.411	0.240
P-IW	best	best	0.466	0.718	0.564
ML	0.454	0.472	0.534	0.843	0.636
BI	0.210	0.092	0.294	0.483	0.352

Bayesian inference

Conversely, the cladogram obtained by BI (Supp. file 6: fig. S1) exhibited a lower resolution than those obtained by parsimony under EW, IW and ML. The cladogram shows that the Lycini are monophyletic (PP = 0.97), and *Rhyncheros* was recovered as polyphyletic, a clade comprising *Rhyncheros* [*R. fuliginosus* (Gorham, 1880), *R. nigrofumosus* (Hinton, 1933), *R. carnifex* (Gorham, 1880) and *R. godmani*] (PP = 0.28) was recovered as early diverging, in a sister position to other Lycini. A second clade of *Rhyncheros* [*R. lineicollis* (Chevrolat, 1834) and *R. sanguinipennis*] (PP = 0.42) was identified as a sister group to remaining members of the Lycini. The clade *Neolycus scutellatus* (Gorham, 1880) + *Rhyncheros sanguineus* (Gorham, 1884) was identified as a sister group to a third *Rhyncheros* clade [*R. rusticus* (Gorham, 1884), *R. fulvellus* (LeConte, 1881), *R. fulvellus femoratus* (LeConte, 1881), *R. simulans* (Schaeffer, 1911), *R. loripes* (Chevrolat, 1834), *R. sagittatus* (Green, 1949) and *R. minutus* (Green, 1949)] (PP = 0.59). *Lycorectus sordidus* gen. et comb. nov. was found in a clade with the other species of *Neolycus*, and *Neolycus* was recovered as a paraphyletic group. The genus *Lycus* was recovered as monophyletic (PP = 0.83), whereas *Lycostomus* was recovered as paraphyletic. Furthermore, *Lycomesus* was identified as the sister group to *Lyconotus*, and the monophyly of *Lyconotus* was well supported (PP = 0.94).

The findings of the implementation of the tree topology tests (Table 2) demonstrated that, among the parsimony-based tree topology tests, the trees generated by parsimony under EW, IW and ML (Table 2; Fig. 8; Supp. file 3: fig. S1, Supp. file 5: fig. S1) outperformed the BI reconstructions (Templeton test, $p > 0.210$; winning-sites test, $p < 0.092$) (Table 2; Supp. file 6: fig. S1). Similarly, among the likelihood-based tree topology tests, the trees generated by parsimony under IW and ML (Table 2; Fig. 8; Supp. file 5: fig. S1) performed better than the parsimony under EW and BI (Table 2; Supp. file 3: fig. S1, Supp. file 6: fig. S1). According to the applied topology tests, trees generated by parsimony under IW (Fig. 8) and ML (Supp. file 5: fig. S1) are not significantly different and are equally plausible (parsimony under IW: Templeton test, best; winning-sites test, best; W-KH, $P > 0.466$; W-SH, $p > 0.718$; AU, $p > 0.564$. ML: Templeton test, $p > 0.454$; winning-sites test, $p > 0.472$; W-KH, $p > 0.534$; W-SH, $p > 0.843$; AU, $p > 0.636$). However, in order to maintain the taxonomic stability of the group (Ferreira *et al.* 2023), the preferred topology is presented, based on parsimony under IW. This topology (Fig. 8) proposes a new classification for North American Lycini, with the genus *Lyconotus* reinstated (Fig. 8) and a new genus, *Lycorectus* (Fig. 8), established. Furthermore, a key is provided to facilitate the recognition of the genera of Lycini in North America, based on the characters that support the groups in the cladogram (Fig. 8; Supp. file 4: fig. S2).

Key to genera of Lycini from North America

1. Length of antennomere III almost the same as antennomere IV (Fig. 4G); head with rostrum longer than wide, but very slender at base; subquadrangular or oval labrum; trochanters with acute internal angle; metatibial spurs short, and acute (Fig. 6F) 2
– Length of antennomere III longer than antennomere IV (Fig. 4E–F); head with rostrum of variable length, but slightly to strongly widened at base; semi-circular to semi-square labrum; trochanters with blunt internal angle; metatibial spurs long, and apically variable shape (Fig. 6G) 3

2. Labrum with truncated anterior margin; in males, last abdominal sternite and phallus are curved at an angle of 45°, without a pair of thorns in the middle part of phallus, without modifications to receive the parameres, which are rounded (Fig. 7E) ..... ***Lycomesus*** Zaragoza-Caballero & González-Ramírez, 2019
– Labrum with rounded anterior margin; in males, last abdominal sternite and phallus are curved at an angle of 90° (Fig. 6P), with a pair of thorns in the middle part of phallus, phallus modified to receive parameres, these are triangular (Fig. 7K) ..... ***Lyconotus*** Green, 1949 stat. rev.

3. Elytra with sexual dimorphism, male considerably dilated in middle part, while female with moderately dilated elytra (Fig. 9D–E); radiomedial loop broadly curved (Fig. 5M); metatibial spurs unequal (inner acute, outer slightly broader apically and bluntly rounded), and situated close together at the base (Fig. 6E) ..... ***Neolycus*** Bourgeois, 1883
– Elytra lacking sexual dimorphism (Figs 9F–G, 10A, 11A); radiomedial loop slightly curved (Fig. 5N); metatibial spurs equal, acute, and with a considerable distance between them at the base (Fig. 6E, G) 4

4. Males with concave or emarginate posterior border on the seventh sternite; thorns on the phallus present or absent (Fig. 7C, F, I) ..... ***Rhyncheros*** LeConte, 1881
– Males with convex posterior border on the seventh sternite; thorns on the phallus absent (Fig. 11C–E) ..... ***Lycorectus*** González-Ramírez & Zaragoza-Caballero gen. nov.

Taxonomy

Class Insecta Linnaeus, 1758
Order Coleoptera Linnaeus, 1758
Superfamily Elateroidea
Family Lycidae Laporte, 1836
Subfamily Lycinae Laporte, 1836
Tribe Lycini Laporte, 1836

Genus ***Lycomesus*** Zaragoza-Caballero & González-Ramírez, 2019
Figs 7E, 9A

Lycomesus Zaragoza-Caballero & González-Ramírez, 2019: 99.

Type species

Lycomesus llorentei Zaragoza-Caballero & González-Ramírez, 2019.

Diagnosis

Lycomesus shares similarities with *Lyconotus*, but it differs in the shape of the anterior margin of the labrum, which is truncated; the presence of a radiomedial loop with sharp edges; the structure of the aedeagus, with parameres that are short and rounded, last abdominal sternite and phallus are characterised

by an angled curvature measuring 45°, as well as the lack of thorns on the phallus. Additionally, the phallus is not modified for the reception of the parameres (Fig. 7E).

Material examined

Refer to Supp. file 1.

Redescription

Body slender. Head concealed by pronotum, rostrum long and slightly widened. Interantennal distance less than 0.09 mm. Antennomere III almost as long as antennomere IV. Labrum semi-square. Mandibles longer than labrum. Pronotum widest at base, with anterior border rounded and anterior margins not prominent, pronotal margin less than 0.52 mm in wide. Elytra with three distinct costae on each elytron (Fig. 9A). Radiomedial loop angle on wing sharp. Trochanters with acute internal angle, metatibial spurs equal and short. Last sternite partially curved. Male genitalia with short, rounded parameres, phallus laterally compressed, slightly widened, and curved at apex (curvature of about 45°), phallus without thorns (Fig. 7E).

Distribution

Lycomesus has only been reported from the type locality in Mexico (Nearctic region) (Zaragoza-Caballero & González-Ramírez 2019).

Genus ***Lyconotus*** Green, 1949 stat. rev.
Figs 4A, C, G, K, V, X, 5D, H, L, O, Q, 6C, F, J, N, P, 7K, N, 9B–C

Lyconotus Green, 1949: 67.

Type species

Lycus lateralis Melsheimer, 1846.

Diagnosis

Similar in appearance to *Lycomesus* (Fig. 9B–C), but differs in the oval shape of the labrum (Fig. 4K); the acute apex of the elytra; the membranous wing with the radiomedial loop slightly acute (Fig. 5O); in males the last sternite and phallus curve at 90°, the thorns of the phallus are modified to receive parameres (Fig. 7K). In the female genitalia, the coxites and valvifers are independent structures, and the outer margin of the coxites cleft is present (Fig. 7N).

Material examined

Refer to Supp. file 1.

Redescription

Body slender. Head concealed by pronotum, rostrum long and very slender (Fig. 4A). Interantennal distance around 0.1–1.12 mm (Fig. 4C). Antennomere III almost as long as antennomere IV (Fig. 4G). Labrum oval (Fig. 4K). Mandibles longer than labrum. Pronotum widest at base, with anterior border rounded and anterior margins not prominent, between 0.53–0.81 mm in width. Elytra without sexual dimorphism, with three distinct costae on each elytron (Fig. 9B–C). Radiomedial loop angle slightly acute (Fig. 5O). Trochanters with acute internal angle (Figs 5Q, 6C), metatibial spurs equal and short (Fig. 6F). Last sternite abruptly curved (Fig. 6P). Male genitalia with long and triangular parameres, phallus slightly widened at base and curved at apex (curvature of about 90°), with transparent keel on ventral part, phallus with thorns modified to receive parameres (Fig. 7K). Female genitalia with slender

stylus, coxites, and valvifers as independent structures, with slender coxites and S shape, valvifers not fused at base (Fig. 7N).

Distribution

Lyconotus is distributed in the Neartic and Neotropical regions. It has been reported in northeastern, southeastern and southern United States as well as in Mexico, Panama, and Colombia (Dugés 1878, 1896; Green 1949; Pérez-Hernández *et al*. 2019; GBIF 2023a).

Genus ***Neolycus*** Bourgeois, 1883
Figs 4B, E–F, M–N, P, R–S, 5C, F, I-K, M, P, R–S, 6B, E, K, M, T, 7A–B, G, J, L, 9D–E

Neolycus Bourgeois, 1883: 61.

Type species

Lycus schoenherri Chevrolat, 1834.

Diagnosis

Neolycus can be distinguished from *Lycomesus*, *Lyconotus*, *Lycorectus* gen. nov., and *Rhyncheros* by the presence of sexually dimorphic elytra, males with elytra considerably dilated in the middle, females with moderately dilated elytra (Fig. 9D–E); membranous wing with the radiomedial loop broadly curved (Fig. 5M); the metatibial spurs unequal, the inner acute, the outer slightly broader apically and bluntly rounded, and situated close to each other at the base (Fig. 6E); the aedeagus with thorns on the phallus (Figs 6T, 7A–B, G, J). In female genitalia, the valvifers are independent structures fused at the base (Fig. 7L).

Material examined

Refer to Supp. file 1.

Redescription

Body slender. Head mostly concealed by pronotum, rostrum variable in length (often very long) (Fig. 4B). Interantennal distance less than 0.09 mm. Antennomere III longer than antennomere IV (Fig. 4E–F). Variable labrum shape (semi-square to rectangular) (Fig. 4M). Mandibles as long as labrum. Pronotum widest at base, with variable anterior border shape (rounded to strongly angulated) (Fig. 4R–S), and anterior margins not prominent, pronotal margin longer than 0.82 mm. Elytra with sexual dimorphism, male with considerably dilated elytra, female with moderately dilated elytra (Fig. 9D–E), both sexes with four distinct costae on each elytron. Radiomedial loop broadly curved (Fig. 5M). Trochanters with rounded internal angle (Figs 5P, R–S, 6B), metatibial spurs unequal (inner acute, outer slightly broader apically and bluntly rounded) and long (Fig. 6E). Male with straight last sternite. Male genitalia with variable shape of parameres (moderately short, or very long and triangular) (Figs 6T, 7A), phallus slightly widened at base and straight to apex (Fig. 7B, G), with a small and transparent keel on ventral part; phallus with thorns of variable length (Figs 6T, 7A–B, G, J). Female genitalia with elongated stylus, coxites, and valvifers as independent structures, with coxites elongated and robust, valvifers fused at base (Fig. 7L).

Distribution

Neolycus is distributed sympatrically with *Rhyncheros* throughout the Neartic and Neotropical regions, with records from southern United States and Mexico (Dugés 1878, 1896; Gorham 1880, 1884; Green 1949; Pérez-Hernández *et al.* 2019; GBIF 2023b), and Peru (Bocak *et al.* 2015).

Genus ***Rhyncheros*** LeConte, 1881
Figs 4D, H–J, T–U, W, 5A–B, E, N, 6A, D, G–I, O, Q–R, 7C, F, H–I, M, 9F–G

Rhyncheros LeConte, 1881: 17.
Thoracocalon Bourgeois, 1883: lxi.

Type species

Lycus sanguinipennis Say, 1823.

Diagnosis

General appearance similar to *Lycorectus* gen. nov. but differs in the shape of the abdominal sternites with acute posterior angles; in males the posterior border of the seventh sternite is concave or emarginate (Fig. 6H–I); aedeagus with parameres of variable length, phallus widened at base, straight to slightly

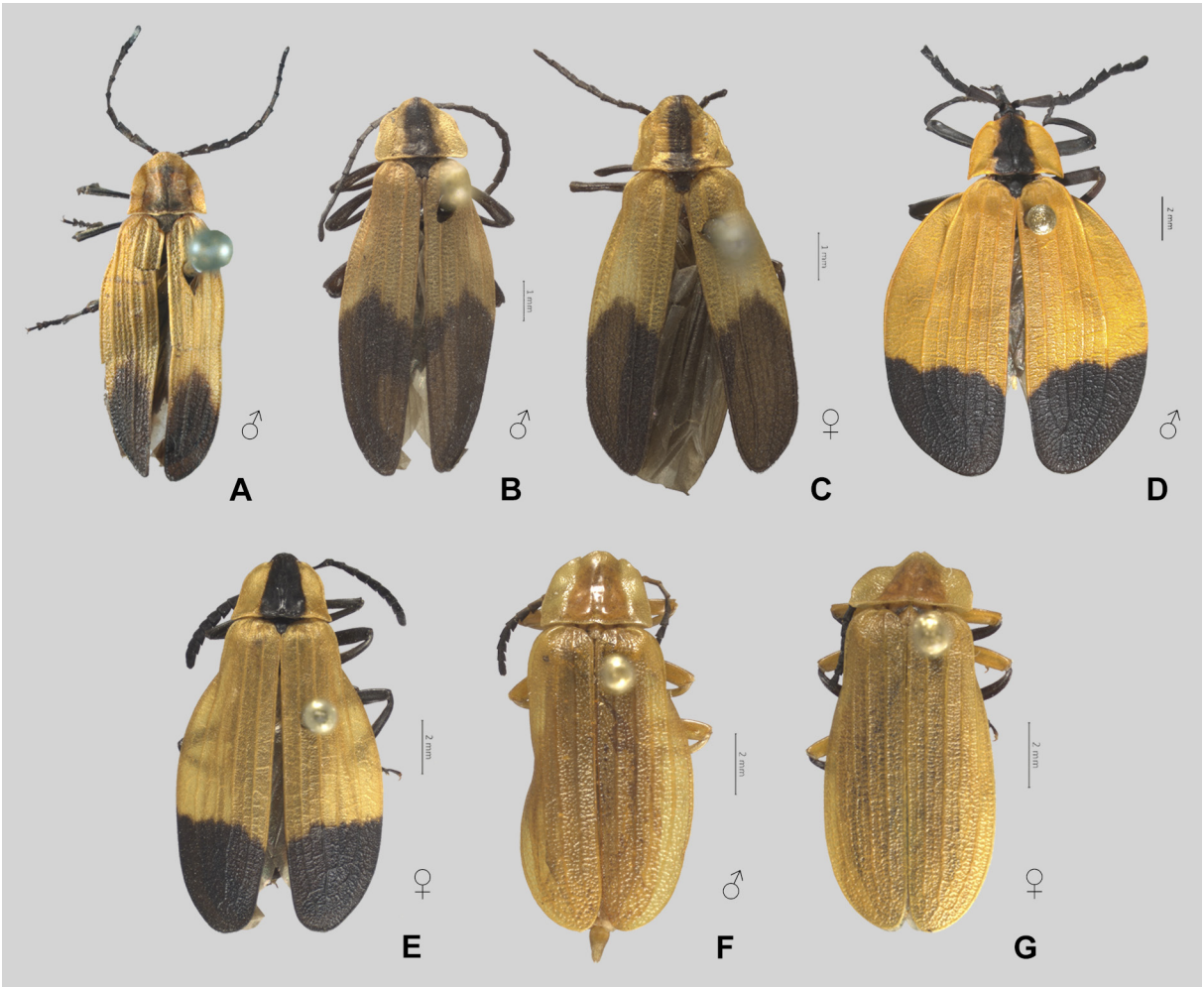

Fig. 9. Dorsal view of the North American Lycini Laporte, 1836. **A**. *Lycomesus llorentei* Zaragoza-Caballero & González-Ramírez, 2019, ♂ (CNIN, QR 70969). **B**. *Lyconotus semiustus* (Chevrolat, 1834), ♂ (CNIN, QR 68732). **C**. *Lyconotus semiustus* (Chevrolat, 1834), ♀ (CNIN, QR 68736). **D**. *Neolycus schoenherri* (Chevrolat, 1834), ♂ (CNIN, QR 67812). **E**. *Neolycus schoenherri*, ♀ (CNIN, QR 67829). **F**. *Rhyncheros loripes* (Chevrolat, 1834), ♂ (CNIN, QR 68174). **G**. *Rhyncheros loripes*, ♀ (CNIN, QR 68175).

curved at apex, in some species, the phallus lacks thorns, in other instances, however, these structures are clearly present (Fig. 7C, F, H–I).

Material examined

Refer to Supp. file 1.

Redescription

Body slender. Head mostly concealed by pronotum, rostrum variable in length (moderately short, often very long) (Fig. 4H–J). Interantennal distance variable in length (less than 0.09 mm to more than 0.13 mm) (Fig. 4D). Antennomere III longer than antennomere IV. Variable labrum shape (semi-circular, semi-square to rectangular) (Fig. 4L). Mandibles as long as labrum. Pronotum widest at base, with variable anterior border shape (rounded to strongly angulated) (Figs 4W, 5A–B), and variable anterior margins shape (not prominent to prominent) (Fig. 4T–U), wide pronotal margin (0.53–0.81 mm, often more than 0.82 mm). Elytra without sexual dimorphism, with four distinct costae on each elytron (Fig. 9F–G). Radiomedial loop slightly curved (Fig. 5N). Trochanters with rounded internal angle (Fig. 6A), metatibial spurs equal, acute and long (Fig. 6D, G). Male with straight last sternite. Male genitalia with variable shape of parameres (moderately long, often short), phallus slightly widened at base, straight to slightly curved at apex, with diminutive and transparent keel on ventral part, phallus thorns may or may not be present and variable in length (Fig. 7C, F, H–I). Female genitalia with variable length of stylus, coxites and valvifers fused, with robust coxites and elongated shape, valvifers not fused at base (Fig. 7M).

Distribution

Rhyncheros is distributed in the Neartic and Neotropical regions. It has been reported in southern United States as well as in Mexico (Dugés 1878, 1896; Gorham 1880, 1884; Green 1949; Pérez-Hernández *et al.* 2019; GBIF 2023b).

Genus ***Lycorectus*** González-Ramírez & Zaragoza-Caballero gen. nov.

urn:lsid:zoobank.org:act:82069CAA-EF3B-4811-915C-44A4EE7F76F0

Figs 10–11

Type species

Lycostomus sordidus Gorham, 1880 (Figs 10–11), by present designation.

Diagnosis

Lycorectus gen. nov. is closely related to *Rhyncheros*. In both genera, the prosternum is strongly carinated, the mesosternum is slightly prominent, the internal angles of the metacoxae are blunt, and the metatibial spurs are equal and long. The main differences between *Rhyncheros* and *Lycorectus* are in the shape of the posterior border of the seventh sternite in males, which may be either concave or emarginate in *Rhyncheros*, but is slightly convex in *Lycorectus*. In addition, the phallus of *Rhyncheros* may or may not have thorns, whereas the phallus of *Lycorectus* lacks thorns (Fig. 10C–E).

Etymology

The name *Lycorectus* is derived from the Greek term '*Lykos*' = 'wolf' and Latin term '*rectus*' = 'straight'. The latter pertains to the straight shape of phallus of the aedeagus in comparison to the same structure in *Lycomesus* and *Lyconotus*.

Description

Body slender. Head mostly concealed by pronotum (Figs 10A, 11A); rostrum long (Figs 10B, 11B); mandibles as long as labrum, straight and slightly curved at apex; antennae of 11 antennomeres; last maxillary and labial palpomere long, distally flattened, and more or less dilated. Pronotum with round anterior margin, wavy posterior margin, straight sides, convex disc. Elytra with four costae that delimit irregular elytral cells. Prosternum strongly carinated; elongated mesothoracic spiracles of tubular shape. Pro- and mesocoxae short and separated; mesosternum slightly protuberant; trochanters with blunt internal angle; metatibial spurs long and equal. Abdominal sternites with slightly pronounced posterior angles; posterior margin of the male seventh sternite slightly convex (Fig. 6L). Aedeagus with short, triangular parameres (in lateral view); straight phallus without thorns (Fig. 11C–E).

Distribution

Lycorectus gen. nov. is distributed in the Neotropical region, and has been reported in Mexico, Guatemala, Nicaragua, and Costa Rica (Gorham 1880, 1884; GBIF 2023b).

Lycorectus sordidus (Gorham, 1880) gen. et comb. nov.
Figs 6L, 10–11

Lycostomus sordidus Gorham, 1880: 5.

Diagnosis

Lycorectus sordidus gen. et comb. nov. is closely related to *Rhyncheros championi*. In both species, the elytra are weakly dilated, and the tibiae are strongly curved. The most notable differences between *R. championi* and *L. sordidus* are observed in the width of the rostrum. In *R. championi*, the rostrum is slender, whereas in *L. sordidus*, it is robust. The length of the antennae differs between the two species. In *R. championi*, the antennae are relatively short, while in *L. sordidus*, they are considerably longer. The width of the macula of the pronotum may be narrow in *R. championi* but is broad in *L. sordidus*. The colouration of the elytra is distinct in the two species. The humeral region and sides of the pronotum of *R. championi* are fulvous, whereas in *L. sordidus*, this colouration is limited to the humeral region. In addition, the colouration of the apex of the femora and the abdomen in *R. championi* is rufo-testaceous, whereas in *L. sordidus* it is dark brown.

Material examined

Syntype

GUATEMALA • ♀; "Calderas, / Guatemala, / Champion // B.C.C. Col. III. (2) / *Lycostomus / sordidus* // (*Lycus*) / *Lycostomus / sordidus*, G // Type // Type. / Sp. figured"; NHMUK 014591974.

Other material examined

COSTA RICA •1 ♂; km 12 Turrialba–Siquirres; 25 Apr. 1984; E. Barrera leg.; CNIN, QR 68429.

MEXICO • 1 ♀; C. Hoffmann leg.; Col. Coleoptera; CNIN, QR 68430.

Redescription

Female (syntype)

Measurements. Length of body 11.22 mm; width 3.63 mm.

Colour. Body slender; general coloration dark brown, except for the sides of the pronotum and the humeral margin of the elytra, which are yellowish (Fig. 10A). Body with dorsal setae fine, short, pubescence yellowish (Fig. 10B).

Head. Prognathous; interocular space concave, integument brilliant and pilose; interantennal distance (0.05 mm) less wide than antennal fossae (0.44 mm); eyes finely faceted, semispherical, not prominent, longer (0.46 mm) than wide (0.30 mm); antennae serrated, long, exceeding beyond posterior coxae, antennomere III longer than antennomere IV; rostrum longer (0.74 mm) than wide (0.55 mm); labrum semi-square, anterior margin straight; mandibles straight, slender and slightly curved at apex, as long as labrum; last maxillary and labial palpomere long, distally flattened, and more or less dilated.

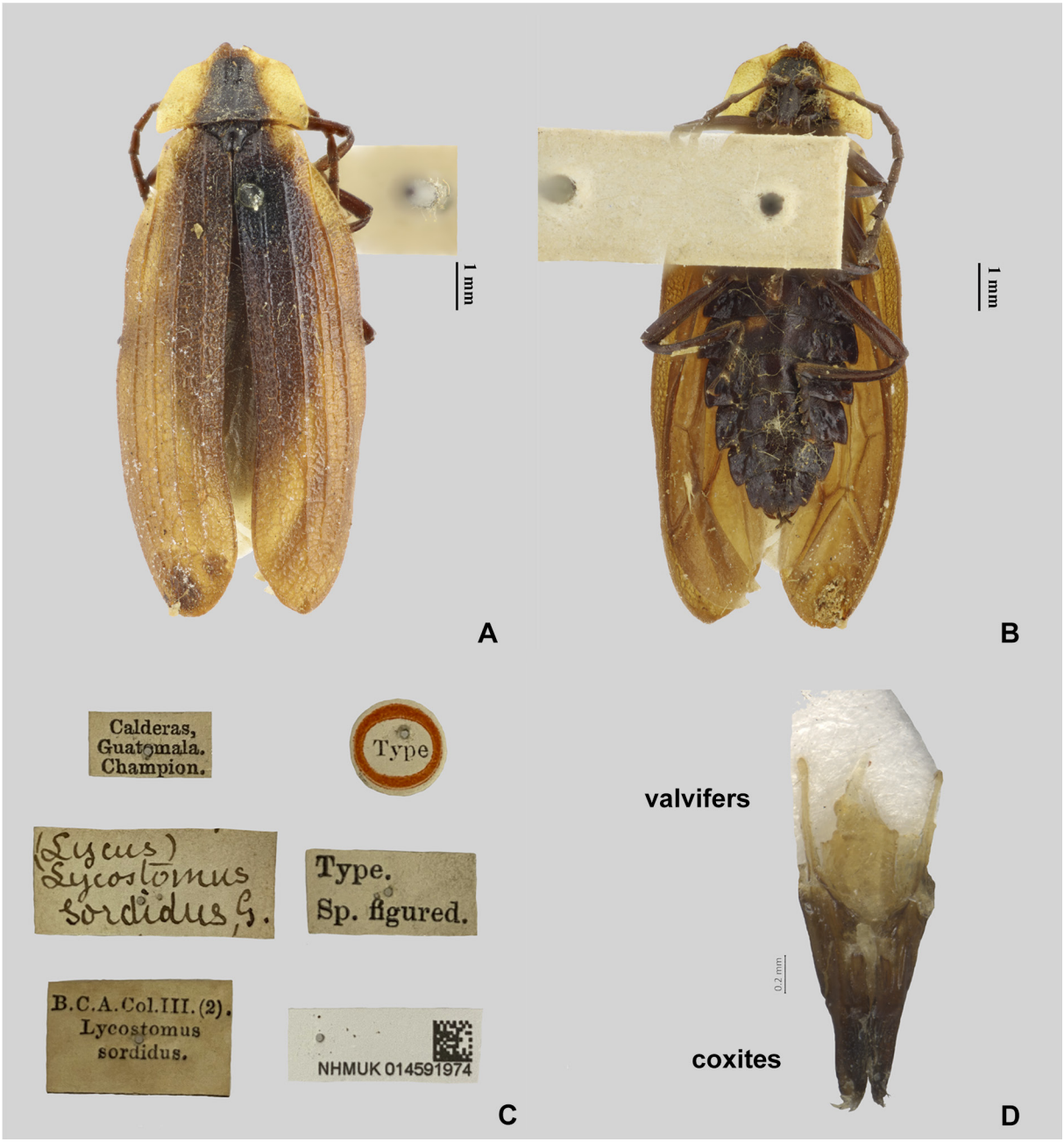

Fig. 10. *Lycorectus sordidus* (Gorham, 1880) gen. et comb. nov., syntype, ♀ (NHMUK 014591974). **A**. General habitus of the adult female in dorsal view. **B**. Ventral view. **C**. Labels (syntype). **D**. Internal genitalia. Photographs: Keita Matsumoto.

Thorax. Pronotum wider (2.96 mm) than long (1.56 mm), subpentagonal, transverse, with roughly dotted surface, anterior and lateral margins widely rounded, pronotal margin 0.80 mm wide, anterior angles non-prominent, decumbent setae; prosternum strongly carinated; scutellum subquadrangular, longer than wide, with emarginated posterior border; elytra long, slightly dilated at base, four times as long (11.36 mm) as wide (2.09 mm), surface rugose, opaque; long legs, pro and mesolegs similar to each other, the metalegs longer, fusiform femurs, tibia channelled, a little dilated at the apex, metatibiae slightly arched, two symmetric tibial spurs long and acute present in pro, meso and meta legs, tarsomeres laterally compressed (0.44 mm), fourth bifid, covering the fifth, claws simple.

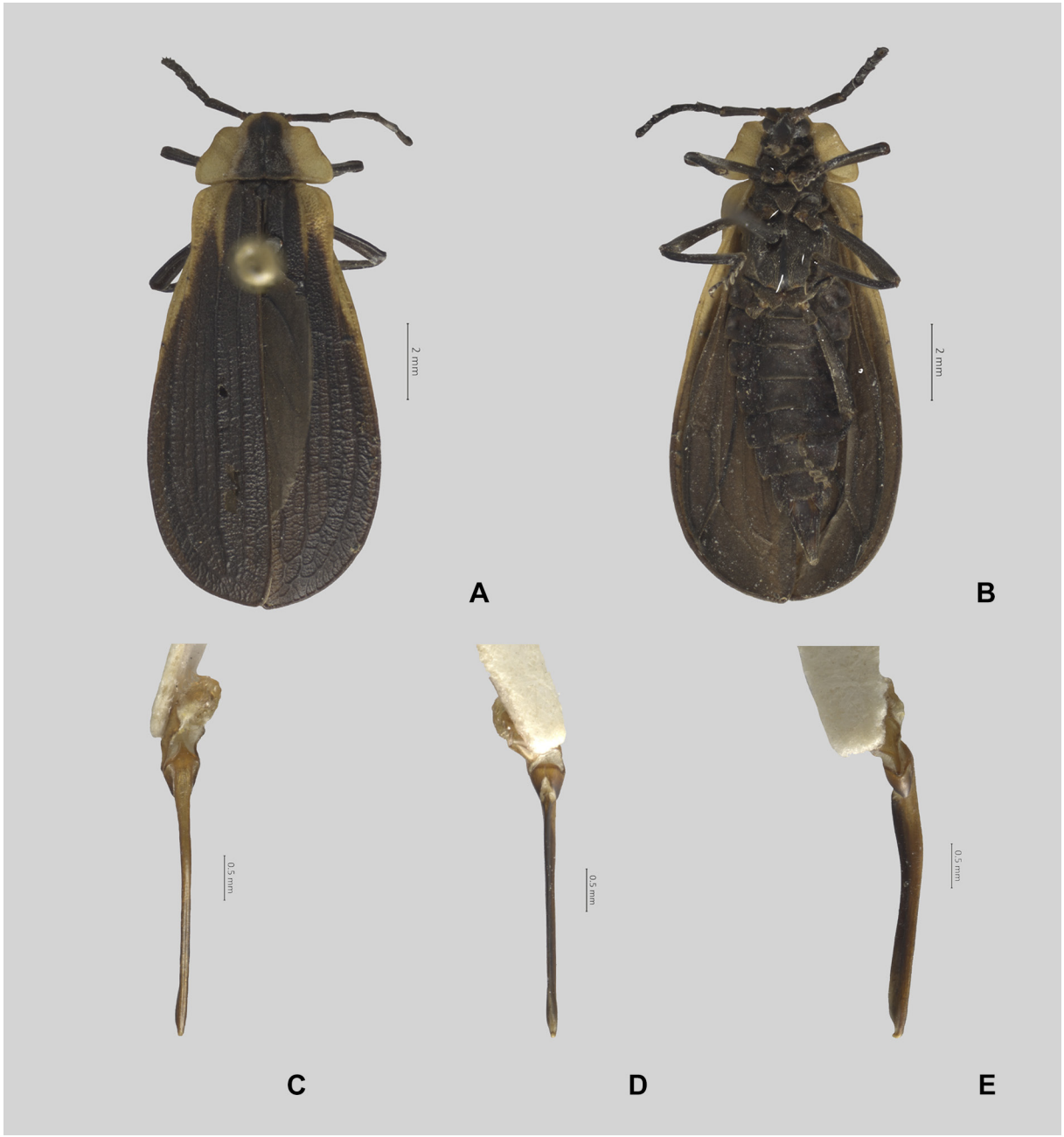

Fig. 11. *Lycorectus sordidus* (Gorham, 1880) gen. et comb. nov., ♂ (CNIN, QR 68429). **A**. General habitus of the adult male in dorsal view. **B**. Ventral view. **C–E**. Aedeagus. **C**. Dorsal view. **D**. Ventral view. **E**. Lateral view.

Abdomen. Abdominal sternites with rounded posterior angles, posterior border of the sixth sternite slightly concave right, last sternite with posterior margin slightly emarginated (Fig. 10B). Ovipositor with stylus elongated, coxites fused to valvifers, coxites slightly longer (1.27 mm) than valvifers (1.04 mm); valvifers divergent posteriorly; proctiger plate long, well-sclerotized (Fig. 10D).

Male

Measurements. Length of body 13.38 mm; width 6.63 mm.

Colour. Body slender; general coloration dark brown, except for sides of pronotum and humeral margin of elytra, which are yellowish (Fig. 11A). Body with dorsal setae fine, short, pubescence yellowish (Fig. 11B).

Head. Prognathous; interocular space concave, integument brilliant and pilose; interantennal distance (0.04 mm) narrower than antennal fossae (0.39 mm); eyes finely faceted, semispherical, not prominent, longer (0.48 mm) than wide (0.30 mm); antennae serrated, long, exceeding beyond posterior coxae, antennomere III longer than antennomere IV; rostrum longer (0.81 mm) than wide (0.5 mm); labrum semi-square, anterior margin straight; mandibles straight, slender and slightly curved at apex, as long as labrum; last maxillary and labial palpomere long, distally flattened, and more or less dilated.

Thorax. Pronotum wider (3.62 mm) than long (2.29 mm), subpentagonal, transverse, with roughly dotted surface, anterior margin rounded, lateral margins straight, pronotal margin of 0.54 mm wide, anterior angles slightly prominent, decumbent setae; prosternum strongly carinated; scutellum subquadrangular, longer than wide, with emarginated posterior border; elytra long, slightly dilated at base, three times as long (11.09 mm) as wide (3.27 mm), surface rugose, opaque; long legs, pro and mesolegs similar to each other, metalegs longer, fusiform femurs, tibia channelled, a little dilated at the apex, metatibiae slightly arched, two symmetric tibial spurs long and acute present in pro, meso and meta legs, tarsomeres laterally compressed, fourth bifid, covering the fifth, claws simple.

Abdomen. Abdominal sternites with rounded posterior angles, posterior border of seventh sternite slightly convex (Fig. 6L), last sternite triangular; aedeagus long, slender, with asymmetrical basal piece (0.93 mm) longer than parameres (0.46 mm) (Fig. 11C), with posterior margin slightly concave, parameres concave, apically slightly acute (Fig. 10E), phallus slender, laterally channelled, median orifice apical, without thorns medially (Fig. 11C–E).

Discussion

Phylogenetic relationships of Lycini

The phylogenetic relationships of the subfamilies and genera of the Lycidae distributed in the Afrotropical, Australian, Oriental, and other Palearctic regions have received increased attention in recent years. These studies have been based on both morphological (Bocak & Bocakova 1990; Bocakova 2001, 2004; Bocak 2002; Kazantsev 2003, 2004a, 2004b, 2006, 2013) and molecular information (Bocak & Bocakova 2008; Bocak & Yagi 2009; Levkanicova & Bocak 2009; Malohlava & Bocak 2010; Kubecek *et al*. 2011, 2015; Sklenarova *et al*. 2013, 2014; Masek & Bocak 2014; Masek *et al*. 2014, 2015, 2018; Jiruskova & Bocak 2015; Li *et al*. 2015a, 2015b, 2017; Uribe & Gutierrez-Rodríguez 2016; Bocek & Bocak 2017, 2019; Kalousova & Bocak 2017; Kusy *et al*. 2017, 2019, 2020; Motyka & Bocak 2018; Bocek & Adamkova 2019; Bocek *et al*. 2019a, 2019b; Jiruskova *et al*. 2019; Bocak *et al*. 2020; Motyka *et al*. 2020, 2021a, 2021b). In contrast, phylogenetic analyses of Lycidae from the Nearctic and Neotropical regions have been limited, exclusively focused on the subfamily Calochrominae Lacordaire, 1857 (Ferreira & Motyka 2023) and the tribes Calopterini and Eurrhacini Bocakova, 2005 (Bocakova 2005; Nascimento *et al.* 2020; Ferreira *et al.* 2023; Nascimento & Bocakova 2024). Recently, Kusy *et al.* (2020) conducted a molecular phylogenetic analysis of the tribe considering Neartic and Neotropical

Table 3. Synapomorphies and homoplastic character states of the major clades in the strict consensus tree obtained under implied weighting.

Clades	Synapomorphies	Homoplastic character states
Lycini	3:2, 5:0, 6:1, 13:0, 31:2, 60:1, 72:5	15:1, 18:0, 19:3, 37:1, 59:2
Lycomesus + *Lyconotus*	55:1, 62:0, 65:1	2:2, 10:2, 57:1
Lycomesus	11:5	21:1, 27:2, 28:1, 32:2, 33:2, 39:0, 50:0, 63:1, 68:0, 70:0
Lyconotus	9:0, 44:2, 49:2, 56:1, 67:4, 72:3, 76:1, 83:3, 85:2, 86:1	1:1, 11:1, 12:1, 25:0, 71:2, 73:1, 78:1, 87:1
Lycus	79:2	2:0, 21:1, 22:1, 26:0, 27:0, 39:0, 44:1
Lycorectus (*Neolycus* + *Rhyncheros*)	36:1, 50:2, 83:2	12:1, 14:1, 32:2, 34:0, 38:0, 66:2, 88:2
Lycorectus	63:5	2:2, 17:0, 23:1, 27:0, 40:2, 42:1, 48:2, 51:2, 53:2, 54:2, 71:1, 72:1, 80:2, 85:1
Neolycus + *Rhyncheros*		10:1, 25:1, 73:1, 80:1
Neolycus	61:1	21:1, 66:1, 83:0, 85:1, 89:1
Rhyncheros	9:1	12:2, 15:2, 16:1, 18:2, 46:1

species; however, they could only include a small sample of American species. Our cladograms obtained under IW and ML (Fig. 8; Supp. file 5: fig. S1), with a larger sample of North American species, differs slightly from that by Kusy *et al.* (2020): *Lycomesus* + *Lyconotus* are sister to the rest of the Lycini (Fig. 8) while in Kusy *et al.* (2020), *Rhyncheros* and *Neolycus*, which are only found in America, formed a clade sister to the other Lycini.

Monophyly of Lycini

Previous studies using molecular evidence have consistently upheld the monophyly of Lycini (Bocak & Bocakova 2008; Bocak *et al.* 2008; Masek *et al.* 2018; Kusy *et al.* 2020). In our analysis it was also supported by seven synapomorphies (Table 3; Supp. file 4: fig. S2). Two of these synapomorphies had already been used to diagnose Lycini: head with rostrum (character 6: state 1) (Fig. 4H–J) and straight mandibles (13:0) (LeConte 1881; Green 1949). Our analysis adds: females with rectangular antennomeres IV–X (character 3: state 2); elongated antennomere III, almost subequal in length to the antennomere IV (character 5: state 0) (Fig. 4G); pronotum with a median longitudinal carina present only at the anterior (31:2); female metatibiae slightly arcuate (60:1); and phallus shape belonging in group 5 (72:5) (Fig. 3). Three of these character states are synapomorphies of Lycini (5:0; 31:2; 72:5), but the diagnostic usefulness of them is limited by several reversals (Supp. file 4: fig. S2). Additionally, the monophyly of Lycini was supported by five homoplastic character states: last maxillary palpomere rectangular, distally flattened, and somewhat dilated (15:1) (Fig. 4N); last labial palpomere rectangular (18:0); palpifer 0.5× longer than prementum (19:3); fusiform cervical sclerites (37:1) (Fig. 5D); and strongly arcuate male metatibiae (59:2) (Fig. 5Q).

Phylogenetic relationships within North American Lycini

For the first time, representatives of three genera of the Lycini in North America have been included in a cladistic analysis. According to our results, the Lycini in North America are now composed of (*Lycomesus* + *Lyconotus*) + (*Lycostomus* + (*Lycus* + (*Lycorectus* + (*Neolycus* + *Rhyncheros*)))) (Fig. 8).

Our results for *Lycus*, *Neolycus* and *Rhyncheros* are consistent with those of Kusy *et al.* (2020); however, they did not include in their analysis the genera *Lycomesus* and *Lyconotus*. Moreover, based on the comparison of the genitalia of the type species of *Rhyncheros* (*R. sanguinipennis*) and *Lyconotus* (*Lycus lateralis*), they considered that both species are closely related and, based on the relationships recovered from Nearctic species, proposed that *Lyconotus* should be considered a junior subjective synonym of *Rhyncheros*.

In our analyses, the genera *Lycomesus* and *Lyconotus* formed a clade that is sister to the other Lycini (Fig. 8). The clade has low statistic support with the analysis of parsimony under IW (BS = 68; JS = 67), but with ML and BI the statistic support was high (UFBoot = 97; PP = 0.99); however, it was supported by three synapomorphies (Table 3; Supp. file 4: fig. S2): males with spinose trochanters (character 55: state 1; Fig. 5Q), short metatibial spurs (62:0; Fig. 6F), and males with last sternite bent medially (65:1). The presence of these characters in the *Lycomesus* + *Lyconotus* clade is indicative of their common ancestry and could be used to differentiate them from *Lycorectus* gen. nov., *Neolycus* and *Rhyncheros* (Supp. file 4: fig. S2). Additionally, the clade was supported by three homoplastic character states: males with rectangular antennomeres IV–X (character 2: state 2; Fig. 4G), labrum longer than wide (10:2), and males with robust metafemora (57:1; Fig. 5Q). The hypothesis that *Lycomesus* + *Lyconotus* are sister to the remaining Lycini (Fig. 8), although with low statistic support, is congruent with the shared morphological features, especially in the genitalia of males (Green 1949; Zaragoza-Caballero & González-Ramírez 2019). It has been reported that, unlike the genitalia of male *Neolycus* and *Rhyncheros*, the genitalia of *Lycomesus* have a curvature of approximately 45° (Zaragoza-Caballero & González-Ramírez 2019) (Fig. 7E), while the genitalia of *Lyconotus* have a curvature of approximately 90° (Green 1949; Zaragoza-Caballero & González-Ramírez 2019) (Fig. 7K).

Lycomesus can be circumscribed by one apomorphic character state (Table 3; Supp. file 4: fig. S2): labrum with truncated anterior margin (character 11: state 5), and ten homoplastic character states (Supp. file 4: fig. S2): prementum with median suture (character 21: state 1), abundant pubescence on lateral margins of pronotum (27:2), pronotal margin width ranging from 0.53 mm–0.81 mm (28:1), pronotum longitudinal areolar wide, spindle-shaped (32:2), abundant pubescence on pronotal disc (33:2), transverse sternellum (39:0), mesosternum not protuberant (50:0), sixth sternite with slightly concave posterior margin on males (63:1), in male genitalia, phallobase as long as parameres (68:0, Fig. 7E), and shape of parameres belonging to morphological group 0 (70:0; Fig. 7E). The present study is the first to evaluate the phylogenetic relationships of *Lycomesus* within the tribe Lycini.

Lyconotus is comprised of two described species; however, during our analysis, we identified four additional species that show significant divergence from *L. lateralis* and *L. semiustus*. The genus presents a greater diversity in the Neotropical region than in the Nearctic region (Supp. file 5: fig. S1) (Dugés 1878, 1896; Green 1949; Pérez-Hernández *et al.* 2019; GBIF 2023a). According to the cladogram, *Lyconotus* has strong statistical support (BS = 84; JS = 88; UFBoot = 95; PP = 0.94) (Fig. 8), and can be circumscribed by ten synapomorphies (Table 3; Supp. file 4: fig. S2, labrum oval (9:0), acute elytral apex (44:2), radio medial loop (49:2; Fig. 5O), females with spinose trochanters (56:1), last sternite of the female undifferentiated (67:4), in male genitalia, phallus has the same shape as group 3 (72:3; Figs 3, 6P, 7K), phallus thorn's structure is adapted to facilitate the reception of parameres (76:1), in the female genitalia, the coxites and valvifers are structures that are non-joined and overlap (83:1; Fig. 7N), coxites with S-shaped (85:2; Fig. 7N), coxites with outer margin cleft (86:1), and a combination of the following character states: interantennal distance ranging from 0.1 mm–0.12 mm (character 1: state 1; Fig. 4C), rounded labrum anterior margin (11:1), semi-rounded lateral margin of labrum (12:1), nearly straight pronotum lateral margins (25:0; Fig. 4V, X), parameres with acute apex (71:2; Fig. 6K), phallus with pair of thorns (73:1), rounded apex of thorns on phallus (78:1), and coxites with distant inner apical margin (87:1). The relationships of *Lyconotus* within the Lycini tribe were assessed here also for the first time.

Our results contrast with those of Kusy *et al.* (2020), who examined the genitalia of the type species of *Rhyncheros* (*R. sanguinipennis*) and *Lyconotus* (*Lycus lateralis*) and suggested them to be closely related. Therefore, after comparing the type species and analysing the relationships between the Nearctic species, they concluded that *Lyconotus* should be regarded as a synonym of *Rhyncheros* (Kusy *et al.* 2020). However, male genital characters have been utilized to distinguish *Lyconotus* from other genera of Lycini (Green 1949; Zaragoza-Caballero 1995; Zaragoza-Caballero & González-Ramírez 2019). Examples of such characters include: parameres about one-third length of the phallus and phallus sharply bent downwards medially (Fig. 7K) (Green 1949; Zaragoza-Caballero 1995; Zaragoza-Caballero & González-Ramírez 2019). Our analysis identified the last character as a synapomorphy supporting the monophyly of *Lyconotus* (Fig. 8). Furthermore, Green (1949) and Zaragoza-Caballero (1995) suggested that additional characteristics, such as the presence of spinose trochanters (Figs 5Q, 6C) and the male last sternite abruptly bent medially (Fig. 6P), can be utilized to distinguish these genera from other North American Lycini. In our analysis, we identified the latter as a synapomorphy that supports the *Lyconotus* clade (Fig. 8). Our phylogenetic analysis corroborates the previous morphological considerations, so we consider *Lyconotus* as a valid genus.

The two analysed species of *Lycostomus* were recovered in distinct clades (Fig. 8): *L. praeustus* was recovered as sister to (*Lycostomus rubrocinctus*) + (*Lycus* + (*Lycorectus* + (*Neolycus* + *Rhyncheros*). Therefore, it would be possible to transfer *L. praeustus* to another genus; however, before making any taxonomic change in this regard, it would be prudent to broaden the sampling of Asian *Lycostomus*. We prefer to wait because Kusy *et al.* (2020) found that the Asian *Lycostomus* represent a monophyletic group.

In our analysis, the genus *Lycus* is sister to the rest of the North American Lycini (Fig. 8). *Lycus* was recovered as monophyletic, with low statistical support; however, it was supported by one synapomorphy (Table 3; Supp. file 4: fig. S2): bifurcated phallus apex (character 79: state 2; Fig. 7D), and a combination of the following homoplastic characters (Supp. file 4: fig. S2): male with bidentate antennomeres IV–X (2:0), prementum with median suture (21:1), angulated anterior margin of pronotum (22:1); punctuated surface on pronotal lateral margin (26:0), sparse pronotal pubescence on lateral margins (27:0), transverse sternellum with posterior rami (39:0), apex of elytra rounded (44:1; Fig. 5G). The support (UFBoot = 91; PP = 0.83) for the monophyly of *Lycus* is consistent with the molecular phylogeny of Kusy *et al.* (2020); however, as with *Lycostomus*, it is necessary to consider a larger sample to analyse the relationships in the genus with greater rigour.

Our cladogram recovered a clade that comprises the remaining North American Lycini (*Lycorectus*, *Neolycus* and *Rhyncheros*). This clade was supported by three synapomorphies (Table 3; Supp. file 4: fig. S2): strongly carinated prosternum (character 36: state 1), strongly protuberant mesosternum (50:2), and fused coxites-valvifers (83:2). Nonetheless, the diagnostic usefulness of theses synapomorphies is weakened by several reversals within the clade (Supp. file 4: fig. S2). The clade was additionally supported by the following combination of homoplastic character states (Supp. file 4: fig. S2): labrum with lateral margins semi-rounded (character 12: state 1), mandible as long as labrum (14:1; Fig. 4L–M), pronotum with wide longitudinal areolar, spindle-shaped (32:2), prosternum not protuberant (34:0), prosternum with rounded posterior border (38:0), female with last sternite cleft (66:2), and coxites longer than valvifers (88:2). The character state of mandibles as long as labrum (14:1; Fig. 4L–M) has an independent origin (with respect to *Lycostomus praeustus*) (Supp. file 4: fig. S2); however, its occurrence within this clade is due to common ancestry.

Lycorectus sordidus gen. et comb. nov. was recovered as sister to *Neolycus* and the other species in the genus *Rhyncheros*. The species *L. sordidus* can be characterized by one apomorphic character (Table 3; Supp. file 4: fig. S2): male six sternite with convex posterior margin (character 63 state 5; Fig. 6L),

and additionally 14 homoplastic characters (Supp. file 4: fig. S2): male with rectangular antennomeres (character 2: state 2), length of fourth maxillary palpomere shorter than second maxillary palpomere (17:0), male pronotum with short anterior angles (23:1), lateral margins of pronotum scarcely pubescent (27:0), elytra dilated towards apex (40:2; Figs 11A), female elytra dilated width-humeral width ratio 1.7 to 2.1 (42:1), bipartite scutellum apex (48:2), narrow mesosternum (51:2), metacoxae inner angle acute in both male and female (53:2; 54:2), in male genitalia, apex of parameres acute (71:1; Fig. 11E), phallus shape as in morphological group 1 (72:1; Figs 3, 11C–E), length of the stylus is greater than 0.30 mm (80:2), and coxites with medial emargination (85:1). Our study is the first to use *L. sordidus* in a phylogenetic context. We proposed the description of a new genus for *L. sordidus* based on the IW topology, which shows it is outside the North American *Rhyncheros* clade; the apomorphic character recovered in our analysis (male convex posterior edge on seventh sternite) (63:5; Fig. 6L) and on the fact that it has been reported for North and South America (Gorham 1880; Pérez-Hernández *et al.* 2019). In the results section, we provide a description for this new genus. Nonetheless, it is imperative to assess the phylogenetic relationships of the South American species of Lycini because *L. sordidus* shares diagnostic characters with *Thoracocalon* (pronotum distinctly rounded in the males and broadly foliated lateral margins), a subgenus that previously included only South American Lycini (Gorham 1880; Bourgeois 1883, 1889, 1901; Pic 1922).

Based on our results, *Neolycus* and *Rhyncheros* are sister taxa (Fig. 8). This group was supported by the combination of the following homoplastic characters (Supp. file 4: fig. S2): labrum wider than longer (character 10: state 1), pronotum with rounded lateral margins (25:1), phallus with pair of thorns (73:1; Figs 6T, 7A–C, F–J), and length of the stylus between 0.22 mm to 0.29 mm (80:1). With respect to thorns on the phallus (character 73: state 1), Kusy *et al.* (2020) considered the absence of thorns in middle part of phallus as a diagnostic character of *Rhyncheros*. We do not support that opinion, because our results showed that this condition was lost in only two species of *Rhyncheros* (*R. nigrofumosus* and *R. loripes*), and hence it is homoplastic (Supp. file 4: fig. S2).

Neolycus is the second most diverse genus of the American Lycini (seven species) and is distributed across both the Nearctic and Neotropical regions. However, its greatest diversity has been recorded in the Neotropical region (Dugés 1878, 1896; Gorham 1880, 1884; Green 1949; Bocak *et al.* 2015; Pérez-Hernández *et al.* 2019; GBIF 2023b). In our IW cladogram, *Neolycus* was recovered as monophyletic although with low statistical support (BS = 59; JS = 64; UFBoot = 80) (Fig. 8). Despite the low support, this result is consistent with the molecular phylogenetic analysis performed by Kusy *et al.* (2020). In our topology, *Neolycus* was supported by one apomorphy (Table 3; Supp. file 4: fig. S2): dissimilar metatibial spurs (the inner spur has an acute apex, while outer spur is slightly broader at apex and bluntly rounded) (character 61: state1; Fig. 6E), and by a combination of the following homoplastic character states (Supp. file 4: fig. S2): prementum with a median suture (21:1), posterior margin of last sternite emarginate (66:1), female genitalia, with coxites and valvifers not joined (83:0); and valvifers fused at base (89:1) (Fig. 7K). We confirm Green's (1949) use of dissimilar metatibial spurs as a diagnostic character for *Neolycus*. The present study is the first to incorporate characters related to female genitalia, although these characters are homoplastic, they add support for the monophyly of *Neolycus* and contribute to the overall resolution of the tree.

According to our topology, *Rhyncheros* is supported as monophyletic, and can be circumscribed by one synapomorphy: labrum semi-circular (character 9: state 1), and by the combination of the following homoplastic characters states (Table 3; Supp. file 4: fig. S2): labrum with rounded lateral margins (12:2), securiform last maxillary palpomere (15:2), fourth maxillary palpomere dilated at the apex (16:1), securiform last labial palpomere (18:2), and spatula-shaped scutellum (46:1). The maxillary palpi character state (15:2) has two independent origins (with respect to *Calopteron* Laporte, 1838) (Supp. file 4: fig. S2). However, its presence within *Lycostomus rubrocinctus* and *Rhyncheros* is a result

of common ancestry. The hypothesis that *Calopteron* is the sister group of Lycini has been proposed by various works (Bocak & Bocakova 1990; Bocakova 2003, 2005; Bocak & Bocakova 2008). This hypothesis is coherent because the larvae of *Calopteron*, *Lycostomus* and *Rhyncheros* share numerous morphological traits, for example, it has been reported that the larvae of these genera have maxillary palpi that are three-segmented and longer than mala (McCabe & Johnson 1979; Bocak & Matsuda 2003; González-Ramírez & Zaragoza-Caballero 2024).

The genus *Rhyncheros* is the most diverse among the American lycines, consisting of 29 species, and is widely distributed in the Nearctic and Neotropical regions (Supp. file 5: fig. S1) (Dugés 1878, 1896; Gorham 1880, 1884; Kleine 1933; Blackwelder 1945; Green 1949; Pérez-Hernández *et al.* 2019; GBIF 2023b). According to Kusy *et al.* (2020) the genus was corroborated as monophyletic and is the sister group to *Neolycus*, and our results support this. Our analysis recovered to *Rhyncheros godmani* as a sister group to other members of the genus *Rhyncheros*. Furthermore, the analysis yielded the identification of two subclades within *Rhyncheros* (Fig. 8). The first is formed by *R. nigrofumosus*, *R. fuliginosus* and *R. carnifex*, which can be characterized by the unique combination of four homoplastic characters (Supp. file 4: fig. S2): labrum with anterior margin emarginate (character 11: state 2), lateral margin of pronotum abundant pubescence (27:2), sternellum V-shaped with short branches (39:2), and males with metacoxae inner angle acute (53:2). The second subclade includes *R. sanguinipennis* (type species) and most of the species in this genus (9): *R. sanguineus*, *R. lineicollis*, *R. fulvellus*, *R. rusticus*, *R. fulvellus femoratus*, *R. simulans*, *R. sagittatus*, *R. loripes*, and *R. minutus*. This group of species can be characterized by the unique combination of four homoplastic characters (Supp. file 4: fig. S2): rectangular labrum in dorsal view (character 9: state 3), prosternum with posterior border truncated (38:1), male elytra dilatated width-humeral width radio less than 1.79 (41:0), and coxites with distant inner apical margin (87:1; Fig. 7M). *Rhyncheros* occurs sympatrically with *Neolycus* in the Nearctic and Neotropical regions (Gorham 1880; Green 1949; Pérez-Hernández *et al.* 2019; Kusy *et al.* 2020).

Our research represents a significant step in the understanding of the evolution of North American lycines, because it incorporates a representative sample of taxa, the largest so far, and incorporates an extensive revision of morphological characters in a phylogenetic context. According to our morphological phylogenetic hypothesis, Lycini are supported as monophyletic. Our results are in a better agreement with a natural classification considering five genera for the North American Lycini, which requires the reinstatement of *Lyconotus*, and the newly proposed genus *Lycorectus*. Ours results extend the classification of North American lycines presented by Kusy *et al.* (2020) to include *Lycomesus*, *Lyconotus*, *Lycorectus* gen. nov., *Neolycus* and *Rhyncheros.*

The phylogeny of North American Lycini is derived exclusively from specimens found in a museum collection, thus highlighting the crucial role of scientific collections in evolutionary studies. Based on the study of this material, the examination of male and female genitalia has yielded a comprehensive understanding of the morphology of North American lycines and offers significant taxonomic value for diagnosing genera. Additionally, the characters obtained from both male and female genitalia provide support and contribute to the resolution of clades in our analysis.

Future research on Lycini should prioritize the utilization of molecular and morphological evidence from North and South American lycines to examine the impacts of alternative data and establish a more robust phylogenetic hypothesis for the South American taxa within Lycini.

Acknowledgments

This paper is part of the requirements for obtaining a Doctoral degree at the Posgrado en Ciencias Biológicas, Universidad Nacional Autónoma de México (UNAM). We thank the Consejo Nacional de Humanidades, Ciencia y Tecnología (CONAHCyT) for the support of this research through funding

and with a graduate scholarship to the first author. We appreciate the help of the curator Michael Geisel for granting us access to the Coleoptera collection at the Natural History Museum (NHMUK). Additionally, we thank Keita Matsumoto and Miriam Aquino Romero for capturing photographs of the type species of Lycini at the NHMUK, to Jon Gelhaus for allowing us access to material of *Rhyncheros sanguinipennis* at the Academy of Natural Sciences in Philadelphia (ANSP), and to Jason D. Weintraub for photographing the specimen; to Chris Grinter and Rachel Diaz-Bastin for providing access to material and photographs of the species *Rhyncheros nigrofumosus* and *Lyconotus lateralis*. We thank Geovanni M. Rodríguez Mirón, Viridiana Vega Badillo, and Francisco Armendáriz Toledano for helping to improve the manuscript. We also thank Susana Guzmán Gómez for technical assistance in taking the photographs. The authors would like to express their gratitude to two anonymous reviewers whose comments have contributed to the enhancement of the work.

References

Blackwelder R.E. 1945 *Checklist of the Coleopterous Insects of Mexico, Central America, the West Indies, and South America*. Bulletin of the United States National Museum, 185. Smithsonian Institution Press, Washington D.C. Available from https://library.si.edu/digital-library/book/bulletinunitedst185161957unit [accessed 20 Oct. 2023].

Bocak L. 2002. Generic revision and phylogenetic analyses of the Metriorrhynchinae (Coleoptera: Lycidae). *European Journal of Entomology* 99 (3): 315–351. https://doi.org/10.14411/eje.2002.043

Bocak L. & Bocakova M. 1990. Revision of the supergeneric classification of the family Lycidae (Coleoptera). *Polskie Pismo Entomologiczne* 59: 623–676.

Bocak L. & Bocakova M. 2008. Phylogeny and classification of the family Lycidae (Insecta: Coleoptera). *Annales Zoologici* 58 (4): 695–720. https://doi.org/10.3161/000345408X396639

Bocak L. & Matsuda K. 2003. Review of the immature stages of the family Lycidae (Insecta: Coleoptera). *Journal of Natural History* 37: 1463–1507. https://doi.org/10.1080/00222930210125362

Bocak L. & Yagi T. 2009 Evolution of mimicry patterns in *Metriorrhynchus* (Coleoptera: Lycidae): The history of dispersal and speciation in Southeast Asia. *Evolution* 64 (1): 39–52. https://doi.org/10.1111/j.1558-5646.2009.00812.x

Bocak L., Bocakova M., Hunt T. & Vogler A.P. 2008. Multiple ancient origins of neoteny in Lycidae (Coleoptera): Consequences for ecology and macroevolution. *Proceedings of the Royal Society B* 275: 215–2023. https://doi.org/10.1098/rspb.2008.0476

Bocak L., Gimmel M.L. & Chaboo C.S. 2015. Beetles (Coleoptera) of Peru: A survey of the families. Lycidae Laporte, 1836. *Journal of the Kansas Entomological Society* 88 (2): 243–247. https://doi.org/10.2317/kent-88-02-243-247.1

Bocak L., Motyka M., Kusy D. & Bilkova R. 2020. Biodiversity inventory and distribution of Metriorrhynchina net-winged beetles (Coleoptera: Lycidae), with the identification of generic ranges. *Insects* 11 (10): 710. https://doi.org/10.3390/insects11100710

Bocakova M. 2001 Revision and phylogenetic analyses of the subfamily Platerodinae (Coleoptera: Lycidae). *European Journal of Entomology* 98 (1): 53–85. https://doi.org/10.14411/eje.2001.010

Bocakoca M. 2003 Revision of the tribe Calopterini (Coleoptera, Lycidae). *Studies on Neotropical Fauna and Enviroment* 38 (3): 207–234. https://doi.org/10.1076/snfe.38.3.207.28169

Bocakova M. 2004. Phylogenetic analyses of the tribe Libnetini with establishment of a new genus (Coleoptera, Lycidae). *Deutsche Entomologische Zeitschrift* 51 (1): 53–64. https://doi.org/10.1002/mmnd.20040510105

Bocakova M. 2005 Phylogeny and classification of the tribe Calopterini (Coleoptera, Lycidae). *Insect Systematics and Evolution* 35: 437–447. https://doi.org/10.1163/187631204788912472

Bocek M. & Adamkova K. 2019. New species of Moluccan trichaline net-winged beetles, with remarks on the phylogenetic position and distribution of *Schizotrichalus* (Coleoptera: Lycidae: Metriorrhynchinae). *Zootaxa* 4623 (2): 341–350. https://doi.org/10.11646/zootaxa.4623.2.8

Bocek M. & Bocak L. 2017. The comparison of molecular and morphology-based phylogenies of trichaline net-winged beetles (Coleoptera: Lycidae: Metriorrhynchini) with description of a new subgenus. *PeerJ* 5: e3963. https://doi.org/10.7717/peerj.3963

Bocek M. & Bocak L. 2019. The origins and dispersal history of the trichaline net-winged beetles in Southeast Asia, Wallacea, New Guinea and Australia. *Zoological Journal of the Linnean Society* 185: 1079–1094. https://doi.org/10.1093/zoolinnean/zly090

Bocek M., Kusy D., Motyka M. & Bocak L. 2019a. Persistence of multiple patterns and intraspecific polymorphism in multi-species Müllerian communities of net-winged beetles. *Frontiers in Zoology* 16: 38. https://doi.org/10.1186/s12983-019-0335-8

Bocek M., Motyka M., Kusy D. & Bocak L. 2019b. Genomic and mitochondrial data identify different species boundaries in aposematically polymorphic *Eniclases* net-winged beetles (Coleoptera: Lycidae). *Insects* 10 (9): 295. https://doi.org/10.3390/insects10090295

Bourgeois J.M. 1883. [Communication]. *Annales de la Société entomologique de France, Bulletin entomologique* 2: LIX–LXII. Available from https://www.biodiversitylibrary.org/page/32549063 [accessed 20 Oct. 2023].

Bourgeois J.M. 1889. Diagnoses de Lycides nouveaux ou peu connus. *Annales de la Société entomologique de France 6e Série* 9: 225–236.
Available from https://www.biodiversitylibrary.org/page/32438777 [accessed 20 Oct. 2023].

Bourgeois J.M. 1901. Les lycides du Muséum d'Histoire naturelle de Paris. *Annales de la Société entomologique de France* 70: 31–51. Available from https://www.biodiversitylibrary.org/page/10012985 [accessed 20 Oct. 2023].

Bourgeois J.M. 1906. Sur le *Celiasis mirabilis* Lacord. [Col.] (note synonymique). *Bulletin de la Société entomologique de France* 11 (8): 95–97.
Available from https://www.biodiversitylibrary.org/page/9486643 [accessed 20 Oct. 2023].

Chevrolat L.A.A. 1834. *Coleóptères du Mexique*. Imprimerie de G. Silbermann, Strasbourg.
https://doi.org/10.5962/bhl.title.47510

De Santis M.D. & Nihei S.S. 2022. Phylogenetic analysis of the tribe Dufouriini (Diptera: Tachinidae) using a total evidence approach based on adult and immature stages. *Arthropod Systematics & Phylogeny* 80: 1–38. https://doi.org/10.3897/asp.80.e69618

Dugès D.E. 1878. Descripción de coleópteros indígenas, (géneros y especies nuevas). *La Naturaleza* 4: 169–188.

Dugès D.E. 1896. *Catálogo de la Colección de Coleópteros Mexicanos formada y clasificada por el Dr. D. Eugenio Dugès (Museo Nacional, Salón de Entomología)*. Imprenta del Museo Nacional, Mexico.

Evenhuis N.L. 2012. François-Louis Comte de Castelnau (1802–1880) and the mysterious disappearance of his original insect collection. *Zootaxa* 3168 (1): 53–63. https://doi.org/10.11646/zootaxa.3168.1.4

Evenhuis N.L. 2023. *The Insect and Spider Collections of the World Webside*. WWW document. Available from http://hbs.bishopmuseum.org/codens/ [accessed 20 Oct. 2023].

Ferreira V.S. & Motyka M. 2023. DNA and morphology corroborate the placement of the former New World *Adoceta* Bourgeois in *Macrolygistopterus* Pic and updates on the status of North American Calochrominae (Coleoptera: Lycidae). *The Coleopterists Bulletin* 77 (1): 63–72. https://doi.org/10.1649/0010-065X-77.1.63

Ferreira V.S., Barbosa F.F., Bocakova M. & Solodovnikov A. 2023. An extraordinary case of elytra loss in Coleoptera (Elateroidea: Lycidae): discovery and placement of the first anelytrous adult male beetle. *Zoological Journal of the Linnean Society* 199 (2): 553–566. https://doi.org/10.1093/zoolinnean/zlad026

GBIF.org 2023a. GBIF Occurrence Download. https://doi.org/10.15468/dl.ftg9r3

GBIF.org 2023b. GBIF Occurrence Download. https://doi.org/10.15468/dl.29r58g

Goloboff P.A. 1993. Estimating characters weights during tree search. *Cladistics* 9 (1): 83–91. https://doi.org/10.1006/clad.1993.1003

Goloboff P.A. 1994. *NONA: A Tree Searching Program*. Program documentation. Published by the author, Tucumán, Argentina.

Goloboff P.A. & Morales M. 2023. TNT version 1.6, with a graphical interface for MacOs and Linux, including new routines in parallel. *Cladistics* 39 (2): 144–153. https://doi.org/10.1111/cla.12524

Goloboff P.A., Carpenter J.M., Arias J.S. & Esquivel D.R.M. 2008. Weighting against homoplasy improves phylogenetic analysis of morphological data sets. *Cladistics* 24 (5): 758–773. https://doi.org/10.1111/j.1096-0031.2008.00209.x

González-Ramírez M. & Zaragoza-Caballero S. 2024. Description of immature stages of *Neolycus* Bourgeois, 1883 and *Rhyncheros* LeConte, 1881 (Coleoptera: Lycidae: Lycinae) from the New World. *Studies on Neotropical Fauna and Environmental* 59 (3): 1250–1264. https://doi.org/10.1080/01650521.2024.2355704

Gorham H.S. 1880. Coleoptera Malacodermata. *In*: Godman F.D. & Salvin O. (eds) *Biologia Centrali-Americana. Insecta. Volume III, Part 2*: 1–7. Taylor & Francis, London. https://doi.org/10.5962/bhl.title.730

Gorham H.S. 1884. Supplement to Malacodermata. *In*: Godman F.D. & Salvin O. (eds) *Biologia Centrali-Americana. Insecta. Volume III, Part 2*: 225–227. Taylor & Francis, London. https://doi.org/10.5962/bhl.title.730

Green J. 1949. The Lycidae of the United States and Canada: I. The tribe Lycini (Coleoptera). *Transactions of the American Entomological Society* 75 (2): 53–70.

Hermes M.G., Melo G.A. & Carpenter J.M. 2014. The higher-level phylogenetic relationships of the Eumeninae (Insecta, Hymenoptera, Vespidae), with emphasis on *Eumenes* sensu lato. *Cladistics* 30 (5): 453–484. https://doi.org/10.1111/cla.12059

Hoang D.T., Chernomor O., Haeseler A., Minh B.Q. & Vinh L.S. 2018. UFBoot2: Improving the ultrafast bootstrap approximation. *Molecular Biology and Evolution* 35: 518–522. https://doi.org/10.1101/153916

Jiruskova A. & Bocak L. 2015. Species delimitation in *Cautires* (Coleoptera: Lycidae) from Peninsular Malaysia using DNA data and morphology. *Annales Zoologici* 65 (2): 239–248. https://doi.org/10.3161/00034541ANZ2015.65.2.007

Jiruskova A., Motyka M., Bocek M. & Bocak L. 2019. The Malacca Strait separates distinct faunas of poorly-flying *Cautires* net-winged beetles. *PeerJ* 7: e6511. https://doi.org/10.7717/peerj.6511

Kalousova R. & Bocak L. 2017. Species delimitation of colour polymorphic *Cladophorus* (Coleoptera: Lycidae) from New Guinea. *Zootaxa* 4320 (3): 505–522. https://doi.org/10.11646/zootaxa.4320.3.6

Kalyaanamoorthy S., Minh B.Q., Wong T.K.F., Haeseler A. & Jermin L.S. 2017. ModelFinder: Fast model selection for accurate phylogenetic estimates. *Nature Methods* 14: 587–589. https://doi.org/10.1038/nmeth.4285

Kassambara A. & Mundt F. 2020. factoextra: Extract and Visualize the Results of Multivariate Data Analyses. R package. Ver. 1.0.7. Available from https://CRAN.R-project.org/package=factoextra [accessed 3 Jan. 2022].

Kazantsev S.V. 2003 Morphology of Lycidae with some considerations on evolution of the Coleoptera. *Elytron* 17: 49–226.

Kazantsev S.V. 2004a. Phylogeny of the tribe Erotini (Coleoptera, Lycidae), with descriptions of new taxa. *Zootaxa* 496 (1): 1–48. https://doi.org/10.11646/zootaxa.496.1.1

Kazantsev S.V. 2004b. Contribution to the knowledge of Macrolycini with description of *Calcaeron*, new genus (Coleoptera, Lycidae). *Zootaxa* 493 (1): 1–32. https://doi.org/10.11646/zootaxa.493.1.1

Kazantsev S.V. 2006. A review and phylogenetic analysis of Afrotropical Dictyopterini (Coleoptera, Lycidae). *Deutsche Entomologische Zeitschrift* 53 (1): 43–64. https://doi.org/10.1002/mmnd.200600005

Kazantsev S.V. 2013. New and little known taxa of "neotenic" Lycidae (Coleoptera), with discussion of their phylogeny. *Russian Entomological Journal* 22: 9–31.

Kleine R. 1933. Lycidae. *In*: Junk W. & Schenkling S. (eds) *Coleopterorum Catalogus, Pars 128:* 1–145. W. Junk, Berlin.

Kubecek V., Dvorak M. & Bocak L. 2011. The phylogenetic structure of Metriorrhynchini fauna of Sulawesi (Coleoptera: Lycidae) with descriptions of a new genus, *Mangkutanus*, and three new species of *Xylobanus*. *Zoological Studies* 50 (5): 645–656.

Kubecek V., Bray T.C. & Bocak L. 2015. Molecular phylogeny of Metanoeina net-winged beetles identifies *Ochinoeus,* a new genus from China and Laos (Coleoptera: Lycidae). *Zootaxa* 3955 (1): 113–122. https://doi.org/10.11646/zootaxa.3955.1.6

Kusy D., Sklenarova K. & Bocak L. 2017. The effectiveness of DNA-based delimitation in *Synchonnus* net-winged beetles (Coleoptera: Lycidae) assessed, and description of 11 new species. *Austral Entomology* 57 (1): 25–39. https://doi.org/10.1111/aen.12266

Kusy D., Motyka M., Bocek M., Masek M. & Bocak L. 2019. Phylogenetic analysis resolves the relationships among net-winged beetles (Coleoptera: Lycidae) and reveals the parallel evolution of morphological traits. *Systematic Entomology* 44 (4): 911–925. https://doi.org/10.1111/syen.12363

Kusy D., Motyka M., Fusek L., Li Y., Bocek M., Bilkova R., Ruskova M. & Bocak L. 2020. Sexually dimorphic characters and shared aposematic patterns mislead the morphology-based classification of the Lycini (Coleoptera: Lycidae). *Zoological Journal of the Linnean Society* 191 (3): 902–927. https://doi.org/10.1093/zoolinnean/zlaa055

Lawrence J.F., Zhou Y.L., Lemann C., Sinclair B. & Ślipiński A. 2021. The hind wing of Coleoptera (Insecta): Morphology, nomenclature and phylogenetic significance. Part 1. General discussion and Archostemata–Elateroidea. *Annales Zoologici* 71 (3): 421–606. https://doi.org/10.3161/00034541ANZ2021.71.3.001

LeConte J.L. 1881. Synopsis of the Lampyridae of the United States. *Transactions of the American Entomological Society and Proceedings of the Entomological Section of the Academy of Natural Sciences* 9 (1): 15–72. https://doi.org/10.2307/25076399

Levkanicova Z. & Bocak L. 2009. Identification of net-winged beetle larvae (Coleoptera: Lycidae) using three mtDNA fragments: a comparison of their utility. *Systematic Entomology* 34 (2): 210–221. https://doi.org/10.1111/j.1365-3113.2008.00457.x

Lewis P.O. 2001. A likelihood approach to estimating phylogeny from discrete morphologic character data. *Systematic Biology* 50 (6): 913–925. https://doi.org/10.1080/106351501753462876

Li Y., Bocak L. & Pang H. 2015a. Molecular phylogeny of *Macrolycus* (Coleoptera: Lycidae) with description of new species from China. *Entomological Science* 18 (3): 319–329. https://doi.org/10.1111/ens.12133

Li Y., Gunter N., Pang H. & Bocak L. 2015b. DNA-based species delimitation separates highly divergent populations within morphologically coherent clades of poorly dispersing beetles. *Zoological Journal of the Linnean Society* 175 (1): 59–72. https://doi.org/10.1111/zoj.12262

Li Y., Pang H. & Bocak L. 2017. The taxonomy of neotenic net-winged beetles from China based on morphology and molecular data (Coleoptera: Lycidae). *Annales Zoologici* 67 (4): 679–687. https://doi.org/10.3161/00034541ANZ2017.67.4.005

Malohlava V. & Bocak L. 2010. Evidence of extreme habitat stability in a Southeast Asian biodiversity hotspot based on the evolutionary analysis of neotenic net-winged beetles. *Molecular Ecology* 19 (21): 4800–4811. https://doi.org/10.1111/j.1365-294X.2010.04850.x

Masek M. & Bocak L. 2014. The taxonomy and diversity of *Platerodrilus* (Coleoptera, Lycidae) inferred from molecular data and morphology of adults and larvae. *ZooKeys* 426: 29–63. https://doi.org/10.3897/zookeys.426.7398

Masek M., Ivie M., Palata V. & Bocak L. 2014. Molecular phylogeny and classification of Lyropaeini (Coleoptera: Lycidae) with description of larvae and new species of *Lyropaeus*. *Raffles Bulletin of Zoology* 62: 136–145. https://doi.org/10.5281/zenodo.5353564

Masek M., Palata V., Bray T.C. & Bocak L. 2015. Molecular phylogeny reveals high diversity, geographic structure and limited ranges in Neotenic net-winged beetles *Platerodrilus* (Coleoptera: Lycidae). *PLoS ONE* 10 (4): e0123855. https://doi.org/10.1371/journal.pone.0123855

Masek M., Motyka M., Kusy D., Bocek M., Li Y. & Bocak L. 2018. Molecular phylogeny and zoogeography of net-winged beetles (Coleoptera: Lycidae). *Insects* 9 (4): 1–18. https://doi.org/10.3390/insects9040154

McCabe T.L. & Johnson L.M. 1979. Larva of Calopteron terminale (Say) with additional notes on adult behaviour (Coleoptera: Lycidae). *Journal of the New York Entomological Society* 87 (4): 283–288.

Melsheimer F.E. 1846. Descriptions of new species of Coleoptera of the United States. *Proceedings of the Academy of Natural Sciences of Philadelphia* 2: 98–118.
Available from https://www.biodiversitylibrary.org/page/6605680 [accessed 20 Oct. 2023].

Minh B.Q., Schmidt H.A., Chernomor O., Schrempf D., Woodhams M.D., Haeseler A. & Lanfear R. 2020. IQ-TREE 2: New models and efficient methods for phylogenetic inference in the genomic era. *Molecular Biology and Evolution* 37 (5): 1530–1534. https://doi.org/10.1093/molbev/msaa015

Motyka M. & Bocak L. 2018. *Escalonius*, a new subgenus of *Calochromus* Guérin Méneville, 1833 identified by the molecular phylogeny of Calochromini (Coleoptera: Lycidae). *Zootaxa* 4461 (1): 77–82. https://doi.org/10.11646/zootaxa.4461.1.5

Motyka M., Bocek M., Kusy D. & Bocak L. 2020. Interactions in multi-pattern Müllerian communities support origins of new patterns, false structures, imperfect resemblance and mimetic sexual dimorphism. *Scientific Reports* 10: 11193. https://doi.org/10.1038/s41598-020-68027-w

Motyka M., Kusy D., Bocek M., Bilkova R. & Bocak L. 2021a. Phylogenomic and mitogenomic data can accelerate inventorying of tropical beetles during the current biodiversity crisis. *eLife* 10: e71895. https://doi.org/10.7554/eLife.71895

Motyka M., Kusy D., Masek M., Bocek M., Li Y., Bilkova R., Kapoitán J., Yagi T. & Bocak L. 2021b. Conspicuousness, phylogenetic structure, and origins of Müllerian mimicry in 4000 lycid beetle from all zoogeographic regions. *Scientific Reports* 11: 5961. https://doi.org/10.1038/s41598-021-85567-x

Nascimento E.A. & Bocakova M. 2024. Phylogenetic analysis reveals a new net-winged beetle genus of Eurrhacini (Coleoptera, Lycidae) from the Pacific slopes of Central America and Ecuador. *ZooKeys* 1204: 241–259. https://doi.org/10.3897/zookeys.1204.114932

Nascimento E.A., Bressan T.D. & Bocakova M. 2020. *Currhaeus*, a new genus of net-winged beetles and phylogenetic analysis of Eurrhacini (Coleoptera: Lycidae: Lycinae). *Zootaxa* 4869 (3): 387–403. https://doi.org/10.11646/zootaxa.4869.3.5

Nixon K. 1999. The Parsimony Ratchet, a new method for rapid parsimony analysis. *Cladistics* 15 (4): 407–414. https://doi.org/10.1111/j.1096-0031.1999.tb00277.x

Nixon K.C. 2002. Winclada ver 1.00.08. Published by the author, Ithaca, New York. Available from https://cladistics.com/downloads [accessed 20 Oct. 2023].

Nixon K.C. & Carpenter J.M. 1996. On consensus, collapsibility, and clade concordance. *Cladistics* 12 (4): 305–321. https://doi.org/10.1006/clad.1996.0023

Pérez-Hernández C.X., Zaragoza-Caballero S. & Romo-Galicia A. 2019. Checklist of net-winged beetles (Coleoptera: Lycidae) from Mexico. *Zootaxa* 4623 (2): 239–260. https://doi.org/10.11646/zootaxa.4623.2.2

Pic M. 1922. Contribution à l'étude des Lycides. *L'Échange* 411: 1–40. Available from https://www.biodiversitylibrary.org/page/57924635 [accessed 4 Mar. 2024].

Rambaut A.A. 2009. FigTree. Tree Figure Drawing Tool. Available from http://tree.bio.ed.ac.uk/software/ [accessed 4 Mar. 2024].

R Core Team 2021. R: A language and environment for statistical computing. R Foundation for Statistical Computing, Vienna, Austria. Available from https://www.R-project.org/ [accessed 3 Jan. 2022].

Rohlf F.J. 2017. TPS Dig2 v.2.31. Ecology & Evolution and Anthropology. Stony Brook University. Available from https://www.sbmorphometrics.org/soft-dataacq.html [accessed 10 Dec. 2023].

Ronquist F. & Huelsenbeck J.P. 2003. MrBayes 3: Bayesian phylogenetic inference under mixed models. *Bioinformatics* 19 (12): 1572–1574. https://doi.org/10.1093/bioinformatics/btg180

Ronquist F., Teslenko M., Van der Mark P., Ayres D.L., Darling A., Höhna S., Larget B., Suchard M.A. & Huelsenbeck J.P. 2012. MrBayes 3.2: Efficient Bayesian phylogenetic inference and model choice across a large model space. *Systematic Biology* 61 (3): 539–542. https://doi.org/10.1093/sysbio/sys029

Sklenarova K., Chesters D. & Bocak L. 2013. Phylogeography of poorly dispersing net-winged beetles: A role of drifting India in the origin of Afrotropical and Oriental fauna. *PLoS ONE* 8: e67957. https://doi.org/10.1371/journal.pone.0067957

Sklenarova K., Kubecek V. & Bocak L. 2014. Subtribal classification of Metriorrhynchini (Insecta: Coleoptera: Lycidae): An integrative approach using molecular phylogeny and morphology of adults and larvae. *Arthropod Systematics & Phylogeny* 72 (1): 37–54. https://doi.org/10.3897/asp.72.e31785

Swofford D.L. & Bell C.D. 2017. PAUP* manual. Available from https://paup.phylosolutions.com/documentation/ [accessed 20 Oct. 2023].

Uribe J.E. & Gutiérrez-Rodríguez J. 2016. The complete mitogenome of the trilobite beetle, *Platerodrilus* sp. (Elateroidea: Lycidae). *Mitochondrial DNA Part B* 1 (1): 658–659. https://doi.org/10.1080/23802359.2016.1219626

Vega-Badillo V., Zaragoza-Caballero S., Ochoterena-Booth H. & Morrone J.J. 2021. Phylogenetic analysis and evolutionary morphology of wings in the genus *Cenophengus* LeConte, 1881 (Coleoptera: Phengodidae: Mastinocerinae) based on morphological characters. *Zoologischer Anzeiger* 293: 168–181. https://doi.org/10.1016/j.jcz.2021.06.007

Wickham H. 2016. ggplot2: Elegant Graphics for Data Analysis. Springer-Verlag, New York. Available from https://www.R-project.org/ [accessed 3 Jan. 2022].

Yang Z. & Rannala B. 1997. Bayesian phylogenetic inference using DNA sequences: A Markov Chain Monte Carlo Method. *Molecular Biology and Evolution* 14 (7): 717–724. https://doi.org/10.1093/oxfordjournals.molbev.a025811

Zaragoza-Caballero S. 1995. Cantharoidea (Coleoptera) de México. II. Lycinae de Veracruz. *Folia entomológica mexicana* 95: 23–84.

Zaragoza-Caballero S. & González-Ramírez M. 2019. Descripción de *Lycomesus llorentei* gen. et. sp. nov. (Coleoptera: Lycini) de San Luis Potosí, México. *Dugesiana* 26 (2): 99–102. https://doi.org/10.32870/dugesiana.v26i2.7075

Printed versions of all papers are deposited in the libraries of three of the institutes that are members of the EJT consortium: Muséum national d'Histoire naturelle, Paris, France; Royal Museum for Central Africa, Tervuren, Belgium; Royal Belgian Institute of Natural Sciences, Brussels, Belgium. The other members of the consortium are: Meise Botanic Garden, Meise, Belgium; Natural History Museum of Denmark, Copenhagen, Denmark; Naturalis Biodiversity Center, Leiden, the Netherlands; Museo Nacional de Ciencias Naturales-CSIC, Madrid, Spain; Leibniz Institute for the Analysis of Biodiversity Change, Bonn – Hamburg, Germany; National Museum of the Czech Republic, Prague, Czech Republic; The Steinhardt Museum of Natural History, Tel Aviv, Israël.

Supplementary files

Supp. file 1. List of specimens examined. https://doi.org/10.5852/ejt.2025.1022.3089.13769

Supp. file 2. Data matrix for phylogenetic analysis of the tribe Lycini Laporte, 1836 (Lycidae: Lycinae). https://doi.org/10.5852/ejt.2025.1022.3089.13771

Supp. file 3. Strict consensus tree of parsimony analysis under equal weight. https://doi.org/10.5852/ejt.2025.1022.3089.13773

Supp. file 4. A single cladogram of parsimony analysis under implied weight. Fig. S1. Unambiguous character changes mapped on branches in WinClada. Fig. S2. Slow optimization using delayed (DELTRAN) transformation. Fig. S3. Fast optimization using accelerated (ACCTRAN). https://doi.org/10.5852/ejt.2025.1022.3089.13775

Supp. file 5. Phylogenetic tree of North American Lycini Laporte, 1836, based on the maximum likelihood analysis. https://doi.org/10.5852/ejt.2025.1022.3089.13777

Supp. file 6. Phylogenetic tree of North American Lycini Laporte, 1836, based on the Bayesian inference. https://doi.org/10.5852/ejt.2025.1022.3089.13781